Technical Bulletin : CSSRI/Karnal/Bulletin/2012/02

Appraisal of Salt Affected, Waterlogged Soils in Rohtak, Bhiwani, Jind and Jhajjar Districts of Haryana Using Remote Sensing and GIS

Madhurama Sethi, M.L. Khurana, Rakesh Bhambri,
D.S. Bundela, S.K. Gupta, Sita Ram, Anil Chinchmalatpure,
S.K. Chaudhari and D.K. Sharma

Central Soil Salinity Research Institute
Karnal 132001, Haryana, India
2012

Technical Bulletin : CSSRI/Karnal/Bulletin/2012/02

Appraisal of Salt-Affected and Waterlogged Soils in Rohtak, Bhiwani, Jind and Jhajjar Districts of Haryana Using Remote Sensing and GIS

Madhurama Sethi, M.L. Khurana, Rakesh Bhambri, D.S. Bundela, S.K. Gupta, Sita Ram, Anil Chinchmalatpure, S.K. Chaudhari and D.K. Sharma

Central Soil Salinity Research Institute
Karnal 132001, Haryana, India
2012

Citation:

Madhurama Sethi, M.L. Khurana, Rakesh Bhambri, D.S. Bundela, S.K. Gupta, Sita Ram, Anil Chinchmalatpure, S.K. Chaudhari and D.K. Sharma. 2012. Appraisal of Salt-Affected and Waterlogged Soils in Rohtak, Bhiwani, Jind and Jhajjar Districts of Haryana Using Remote Sensing and GIS. Central Soil Salinity Research Institute, Karnal-132 001 (Haryana), India. Technical Bulletin : CSSRI/Karnal/2012/2, pp28.

Published by:

Director, Central Soil Salinity Research Institute,
Zarifa Farm, Kachhwa Road, Karnal-132 001 (Haryana), India.
Telephone : +91-184-2290501; Fax : +91-184-2290480, 2292489
E-mail : director@cssri.ernet.in; sethim@cssri.ernet.in
Website : www.cssri.org

Technical Assistance:

Randhir Singh

Front Cover Page Photo:

A view of Salt Affected Soil of Rohtak District of Haryana

Printed at:

Glam Media
SCO - 3, Level - II, Sector - 8, Karnal - 132 001
E-mail : glam.media@gmail.com

Contents

Appraisal of Salt-Affected and Waterlogged Soils in Rohtak, Bhiwani, Jind and Jhajjar Districts of Haryana using Remote Sensing and GIS

INTRODUCTION

Soil salinity is a major hazard to agriculture and water resources, restricting food production in many countries of the world. In India, soil salinity is a problem that generally occurs in the arid, semiarid regions and canal command areas. The accessible database over the country for salt affected soils and their classification is limited and scattered due to the variability of salinity/alkalinity levels in the field and an absence of uniformity in criterion that define identification and inventory. Furthermore, statistics about the total area in the country provided by different government agencies do not match (Singh et al. 2009). A suitable and accurate method is required for identification monitoring and mapping of soil salinity in order to check the threat to normal lands for effective management and amelioration of salty lands.

A conventional survey demands a great deal of time and capital for mapping, whereas innovative geoinformatics techniques provide abundant potential for mapping and monitoring a larger coverage of soil salinity at regular intervals (Lu et al., 2004). Mapping and monitoring of soil salinity is required to establish its areal extent and also to keep track of changes in salinity in order to formulate appropriate and timely management strategies for reclamation and rehabilitation of salt affected soils. Geographical Information System (GIS) tools facilitate the complex studies of soil hazards such as soil salinity/sodicity and help to manage a great set of variables and a huge amount of spatial data. In addition, data on rainfall, topography, soil type and other spatial information which affect or lead to soil salinity can be analyzed using GIS to determine spatial patterns of salinisation and to predict regions that may be at risk. Remote sensing data have been extensively used in soil-salinity studies as they are not only quicker but are also precise and accurate, therefore, useful for making realistic predictions. Several studies based on remote sensing proves that application of remote spectral sensors in soil salinity mapping can directly define salinity from bare soil and indirectly from vegetation in real-time and in a cost-effective manner for large-area monitoring (Sharma and Bhargava, 1988; Metternicht and Zinck, 2003). The lack of vegetation or scattered vegetation on salt-affected soil surfaces also makes it possible to detect areas affected by soil salinity (Metternicht and Zinck, 2003). A variety of remote-sensing data has been used for identifying, mapping and monitoring salt-affected areas, including aerial photographs, video images, and infrared thermography, visible, infrared multispectral and microwave images (Metternicht and Zinck, 2003). Some studies identify most suitable bands of sensors for saline soil mapping. Menenti et al. (1986) established that Landsat Thematic Mapper (TM) bands 1, 5 and 7 were better for identifying salt minerals, when they are a dominant soil ingredient. Saha et al. (1990) and Madrigal et al. (2003) detected soil salinity of cropped areas by correlating soil EC determined at point sites within previously selected fields, to spectral values extracted from bands 2, 3 and 4. Venkataratnam (1983) used MSS images of pre-monsoon, post-monsoon and harvest seasons to map soil salinity in the Punjab. He concluded that the spectral curves of highly and moderately saline soils change considerably during the annual cycle, which significantly complicates the time-compositing procedure. Salt affected waterlogged soils were mapped by Sethi et al. (1996) in the Ukai-Karapar command area using IRS images, visual interpretation and ground truth. The salt affected soils of Kanpur district were mapped using IRS IB imagery on 1:50,000 scale by Sethi et al. (2001). Recently salt affected and waterlogged lands were mapped in South West Punjab (Sethi et.al, 2004) where a comparison of 1997 and 2001 May and February images were processed using image processing, additional ground truth, geomorphological analysis, image processing and GIS (ERDAS & ARCINFO). It was found that almost 42 % of the area was at high risk of salinisation. It is apparent that most studies converge on trying to find an effective way to identify and study salinity from remote sensing data. The multiplicity of techniques and methodologies adopted so far over the country have all been attempts at gaining some level of accuracy and grappling with the issues of variability.

The focused goals of the present study were (1) development of a simple and robust technique for soil salinity mapping using remote sensing and GIS technology and (2) estimation of salt affected area in Rohtak, Jhajjar, Bhiwani and Jind Districts of Haryana using remote sensing satellite data, ground truth and geo-informatics (Fig. 1).

METHODOLOGY

Maps, Satellite Data and Rectification

Satellite images of IRS P6 dated October 2006 and Feburary 2007 were acquired from National Remote Sensing Centre (NRSC, http://www.nrsa.gov.in). The global DEM derived from ASTER data (GDEM) tiles were directly downloaded for our study area. The global DEM has been derived from ASTER data (GDEM) which was released in July 2009 and is freely available from the Japanese Earth Remote Sensing Data Analysis Center (ERSDAC) at http://www.gdem.aster.ersdac.or.jp/. A total of 33 Survey of India topographic sheets on 1:50000 scale, were used for the preparation of the base maps (Fig. 2).

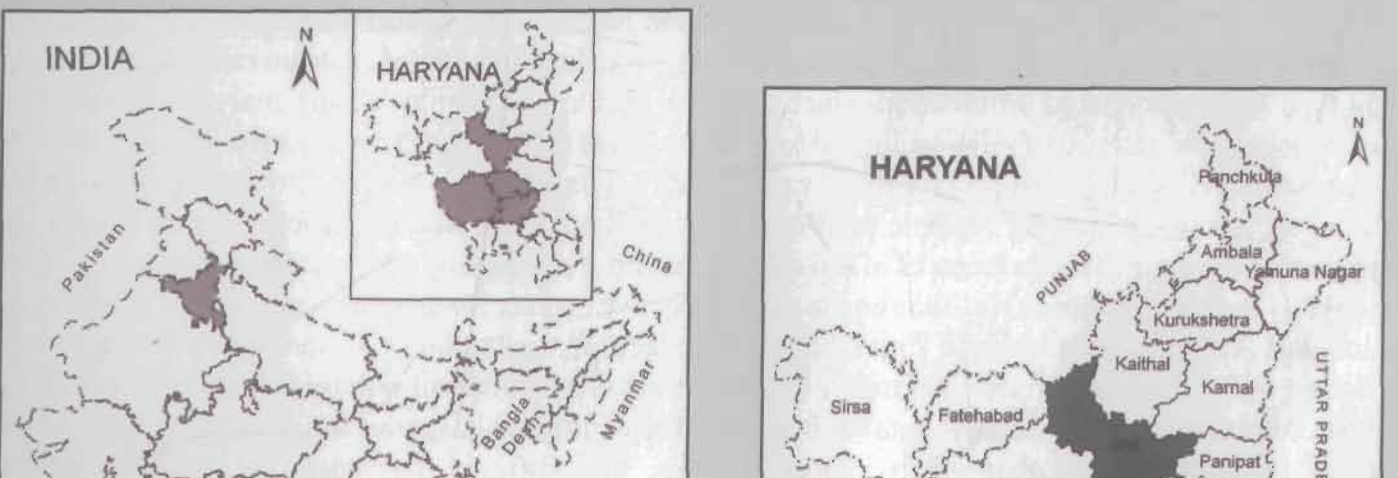

Fig. 1 : Location of districts in Haryana

The IRS P6 Satellite images were rectified based on SOI image and GDEM- DEM data using rectification techniques and projective transformation in ERDAS Imagine 9.3. We used 84 ground control points (GCPs) for rectification and found a root mean square error (RMSE) of 0.6 pixels. It was observed during the interpretation of the SOI map of 1960s that the area marked as scrub land actually represented salt affected areas as interpreted on the 2006 IRS-P-6 images. When the former was overlaid on the latter it was very clear that the two areas merged. The area reclaimed since 1960s could also be accurately identified. To add more information to the database, a vector base map of landuse features such as canals, roads, and drainage were composited for the study area based on satellite image and visual interpretation. This was further cross validated with the SOI map (Fig. 2).

Satellite data was interpreted for demarcation of salt affected patches. The spatial resolution of the data was

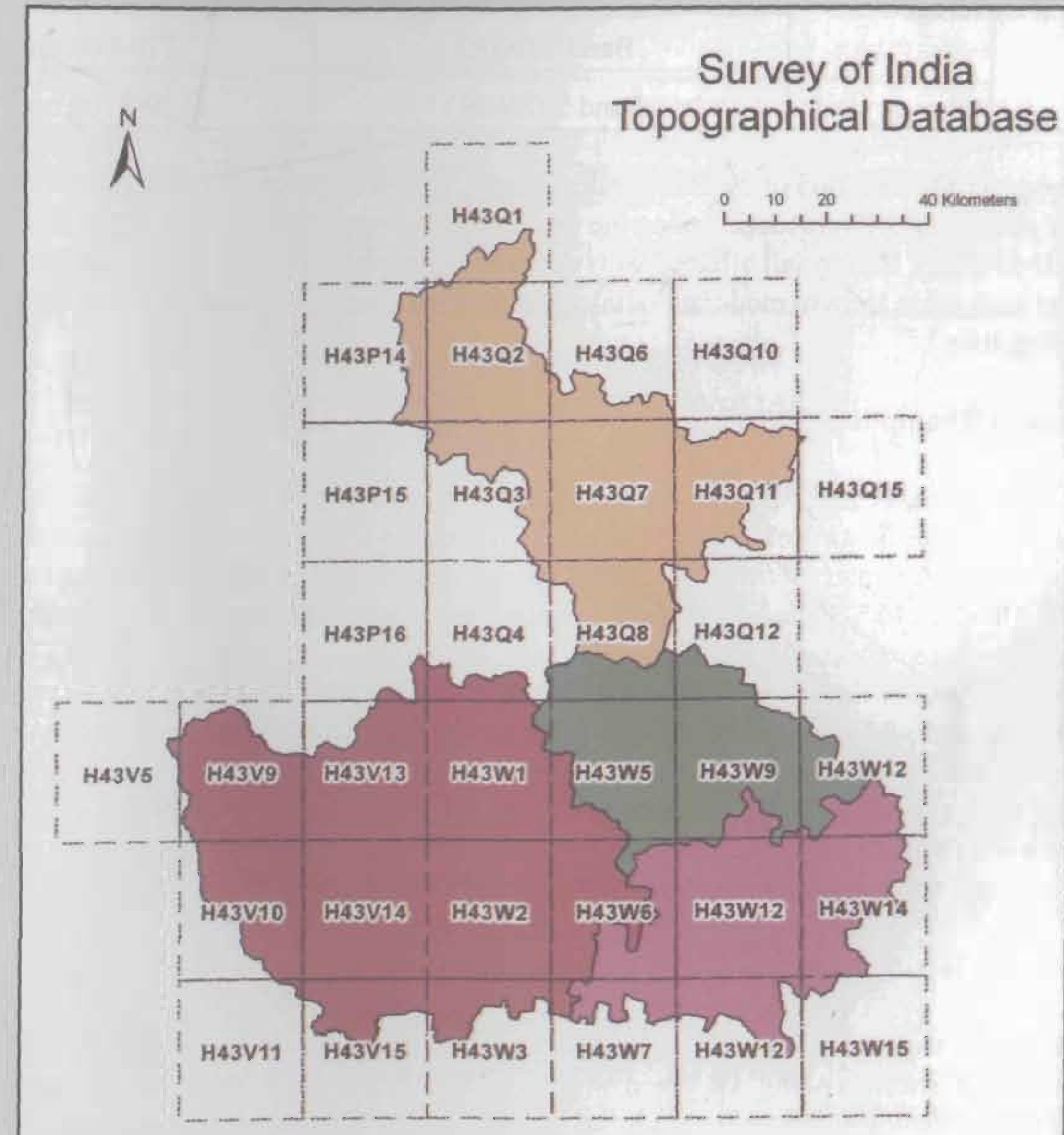

Fig. 2 : Survey of India topographical sheets

Table 1: Key Parameters of IRS-P6 LISS III sensor

BANDS		
Spatial Resolution	Band 2 (green)	23.5 m
	Band 3 (red)	23.5 m
	Band 4 (NIR)	23.5 m
	Band 5 (SWIR)	23.5 m
Spectral Coverage	Band 2 (green)	520-590 nm
	Band 3 (red)	620-680 nm
	Band 4 (NIR)	770-860 nm
	Band 5 (SWIR)	1550-1700 nm

23.5 m. and the spectral resolution of the Bands ranged from 520nm in the green band to 1700 nm in SWIR (Table 1). Salt affected soils were identified on the false colour composite of bands 4 (770-860 nm), 3(620-680 nm), 2(520-590 nm). Barren salt affected soils appear as light blue and white on the images. They also appear mottled with red in areas of moderate salinity and dark blue to grey in areas where water-logging and salinity occur together.

Field Work and Soil Sampling

Field work was executed based on the information which was gathered from visual interpretation and the initial digital rectification of satellite images. Soil samples were collected from bare fields using a soil auger from every 2 km interval from most of the accessible areas in the districts after the harvest of rice from depths of 0-15 and 15-30cms. Deep core sampling was carried out at a depth of 30-60cms and 60-120cms from different representative sites.

To acquire location details of each sample site, Global Positioning System (GPS) readings were acquired using the hand-set Garmin Etrex GPS units. Even though the GPS was not differentially accurate, the hand-held Garmin GPS instrument is useful in providing a fairly accurate source of ground control points (GCPs) with expected vertical accuracies in the order of ±15m (Racoviteanu et al. 2007) and horizontal accuracies of ±3.9 m .(Ackerman et al. 2001). We estimated a horizontal accuracy of ±6 to 10 m which was displayed on the GPS screen, each time depending on the number of satellite signals received.

Supervised Image classification

Initially an unsupervised classification was carried out using ISODATA in ERDAS IMAGINE on the complete image encompassing all the districts. The first iterations were run to create clusters. Subsequently the number of iterations was reduced and the classes identified for input in the creation of the supervised classification. Individual samples for each class were identified and analyzed for reflectance values and spectral profiles of major soil types were generated using ERDAS Imagine 9.3. Ground sample analysis of soil samples from all the districts formed the integral basis for classification and creation of the spectral profile and classification.

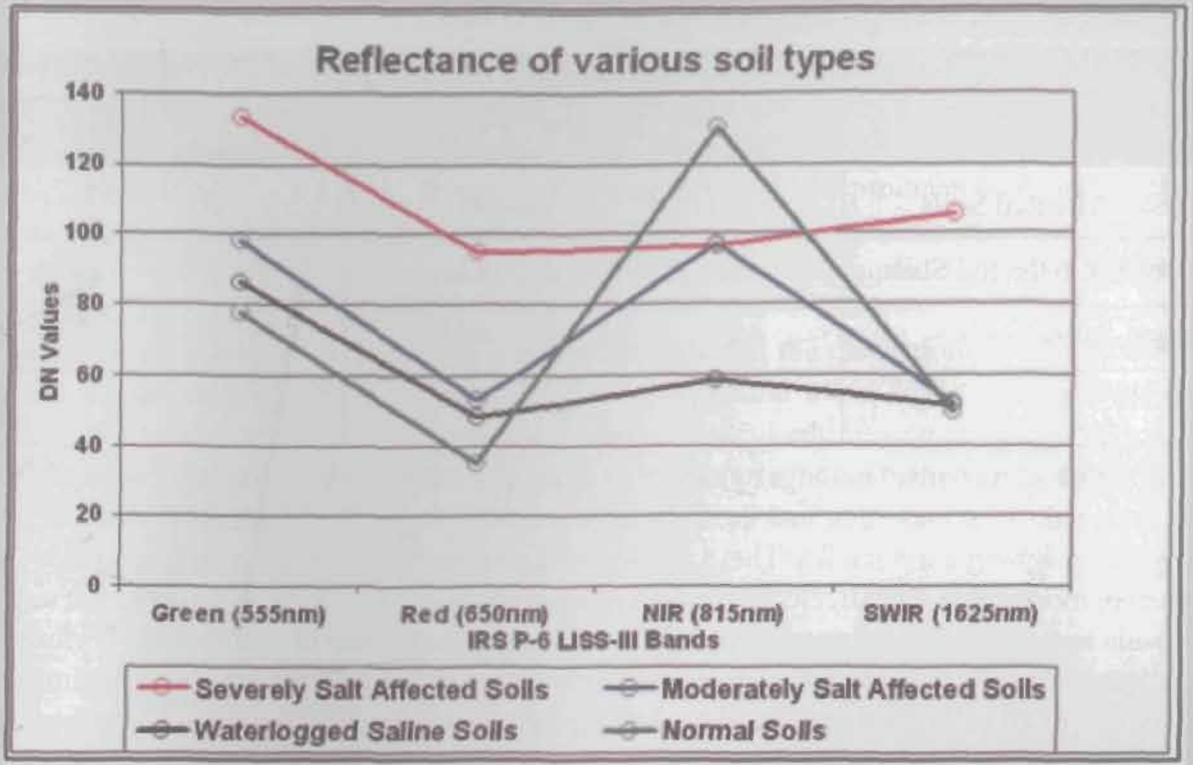

Fig. 3: Spectral signatures of soils in different bands

A spectral profile was created to represent various types of salt affected soils, moderately salt affected soils, waterlogged and saline soils and vegetation using the IRS P6 LISS III image. The averages DN values of spectral profiles of each class were calculated separately for clarity.

It was observed that all soils had higher a reflectance in the Green band (0.555µm) with salt affected soils reflecting the maximum (Fig. 3) followed by moderately salt affected soils. The lower reflectance of moderately salt affected soil in the red and SWIR region is where the soils have a vegetative cover.

Waterlogged saline soils also had a lower reflectance because of the presence of moisture in the Red, NIR and the SWIR region. Vegetation peaked in the NIR region due to the greeniness of the vegetation. Reflectance of vegetation however, was low in the red, green and SWIR regions of the spectrum because of the absorption of chlorophyll for photosynthesis. It is noticeable that the reflectance from healthy green vegetation increases dramatically as we reach the near infrared portion of the spectrum. In the near infrared (NIR) region, the reflectance is much higher than that in the visible band due to the cellular structure in the leaves (www.crisp.nus.edu.sg.).

It was found that reflectance of all soils was considerably lower in the red band (0.65µm) however severely salt affected soils had a high reflectance in all the bands equally because of poor or no vegetation cover. Moderately salt affected soils had a lower reflectance along with green vegetation in the red band of the spectrum (Table 2). The reflectance in the near-infrared plateau varied with vegetation type, water content, and canopy architecture. In contrast, bare salt affected soil had approximately the same reflectance in both the visible and near-infrared portion of the spectrum. The reflectance characteristics in the visible and the near infrared bands have been used to monitor vegetation in the multispectral remote sensing images.

Based on the spectral signatures and the established range, training sites were decided for different classes for supervised classification using the Maximum Likelihood Classification. The Maximum Likelihood Classification assumes that the statistics for each class in each band are normally distributed and calculates

Table 2 : Average spectral profile of different soils in different bands

Soil Types ↓	Green (0.555μm)	Red (0.65μm)	NIR (0.815μm)	SWIR (1.625μm)
Severely Salt Affected Soils	133	95	96	106
Moderately Salt Affected Soils	98	53	97	52
Waterlogged Saline Soils	86	48	58	51
Normal Soils	78	35	130	50

the probability that a given pixel belongs to a specific class. (Richards, 1999) All pixels were classified and each pixel assigned to the class that had the highest probability hence the clusters created had maximum separability for assigning class names. These classes included normal soils with agriculture, severely salt affected barren, moderately salt affected soils with agriculture, sand, waterbody, settlements, waterlogged and saline soils with agriculture. Supervised classification with maximum likelihood was performed based on these training sites. We found that roads were misclassified as saline soils therefore assuming that the roads had a width of 10 m, buffers were generated along the roads. The classified image was then converted into vector (polygon) database. Misclassified roads were clipped from the classified vector database using the clip algorithm of GIS overlay operation based on ArcGIS to eliminate the misclassification and subsequently remove the error (Fig. 4 a & b).

Classification accuracy assessment

To study the accuracy of the classification an accuracy assessment of the classified maps was carried out using an error matrix based on accuracy measures (Congalton, 1991). The digital image of Febuary 2007 of LISS III was selected as a reference image for assessing the accuracy of the image classification which was used in previous study by Sethi et al. (2004). Ground soil sample details as before were the basis of the final classification process, selection of pixels and accuracy assessment.

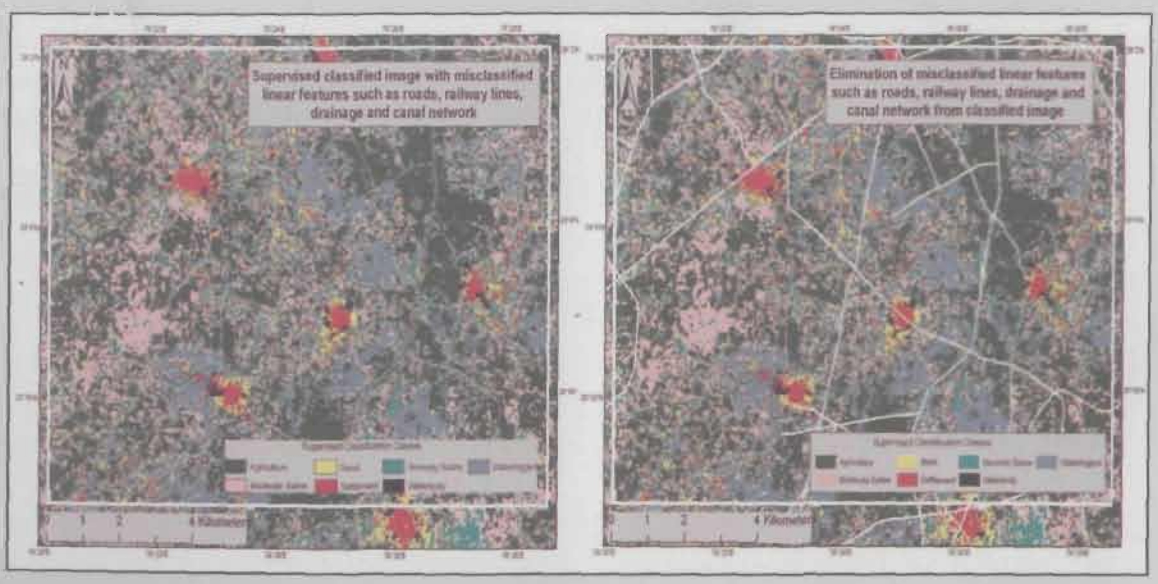

Fig. 4: (a) Supervised classification with misclassified linear features; (b) elimination of misclassified linear features.

The 50 testing pixels were collected in equalized random fashion from the classified LISS III image per class. The error matrix generated could be utilized to determine the over-all accuracy of the map and individual class accuracies in the form of user's and producer's accuracies (Congalton, 1991). The overall accuracy was then used to indicate the accuracy of the whole classification (i.e. the number of correctly classified pixels divided by the total number of testing pixels). The producer's accuracy relates to the probability that a reference sample was correctly mapped, and measures the omission error. The user's accuracy indicates the probability that a sample from the classified map actually matches what it was in the reference data, and measures the commission error.

The error-matrix based accuracy assessment reveals that the methodology applied here has been quite successful in mapping and isolating salt affected soils and other land-cover classes. The *Kappa* statistic applied reflects the difference between actual agreement and the agreement expected by chance Kappa of 0.85 means there is 85% better agreement than by chance alone. Kappa is computed as

$$k = \frac{N\sum_{i=1}^{r} x_{ii} - \sum_{i=1}^{r}(x_{i+} \times x_{+i})}{N^2 - \sum_{i=1}^{r}(x_{i+} \times x_{+i})}$$

Where :

N - Total number of sites in the matrix

r - Number of rows in the matrix

xii - Number in row *i* and column *I*

x_{+i} is the total for row *I*, and

x_{i+} is the total for column I (Jensen 1996).

The producer's accuracies for all classes in table 3 were above 80% except in moderately salt affected soils with agriculture where it was 73.21%. In the users accuracy again the accuracy levels were more than 80% but was only 76% in severely salt affected barren soils. These errors occurred due to misclassification of the pixels. The overall accuracy of the maximum liklihood classfication using the accuracy assessemnt matrix was 87.25 percent using the KHAT coefficient.

Table 3 : Accuracy assessment for landuse classes in Rohtak District.

Class Name	Reference Totals	Classified Totals	Number Correct	Producers Accuracy	Users Accuracy
Unclassified	52	50	50	---	---
Sand	45	50	43	95.56%	86.00%
Severely salt affected/barren	43	50	38	88.37%	76.00%
Settlement	52	50	45	86.54%	90.00%
Normal soils/Agriculture	51	50	43	84.31%	86.00%
Waterbody	47	50	45	95.74%	90.00%
Moderately salt affected	56	50	41	73.21%	82.00%
Waterlogged and saline soils	54	50	44	81.48%	88.00%
Total	400	400	349		
Overall Classification Accuracy =	**87.25%**				

ROHTAK DISTRICT

Rohtak district of Haryana state of India covers nearly 1745 km2 (Fig. 5) and is located between 28° 23'and 29°06'N latitude and 76°13' to 76 ° 58' E longitudes. The physiography is gentle plain ranging from 215 m to 222m above msl. Undulating sandy dunes mark the overall topography of the district. The average elevation of the district is about 220 meters above mean sea level. There is gentle slope of about 19 cm. per kilometre from north-east to south-west. The hydrologic gradient of ground water is very gentle. The climate is subtropical monsoon with an average annual rainfall of 592 mm, most of which occurs from June to September.

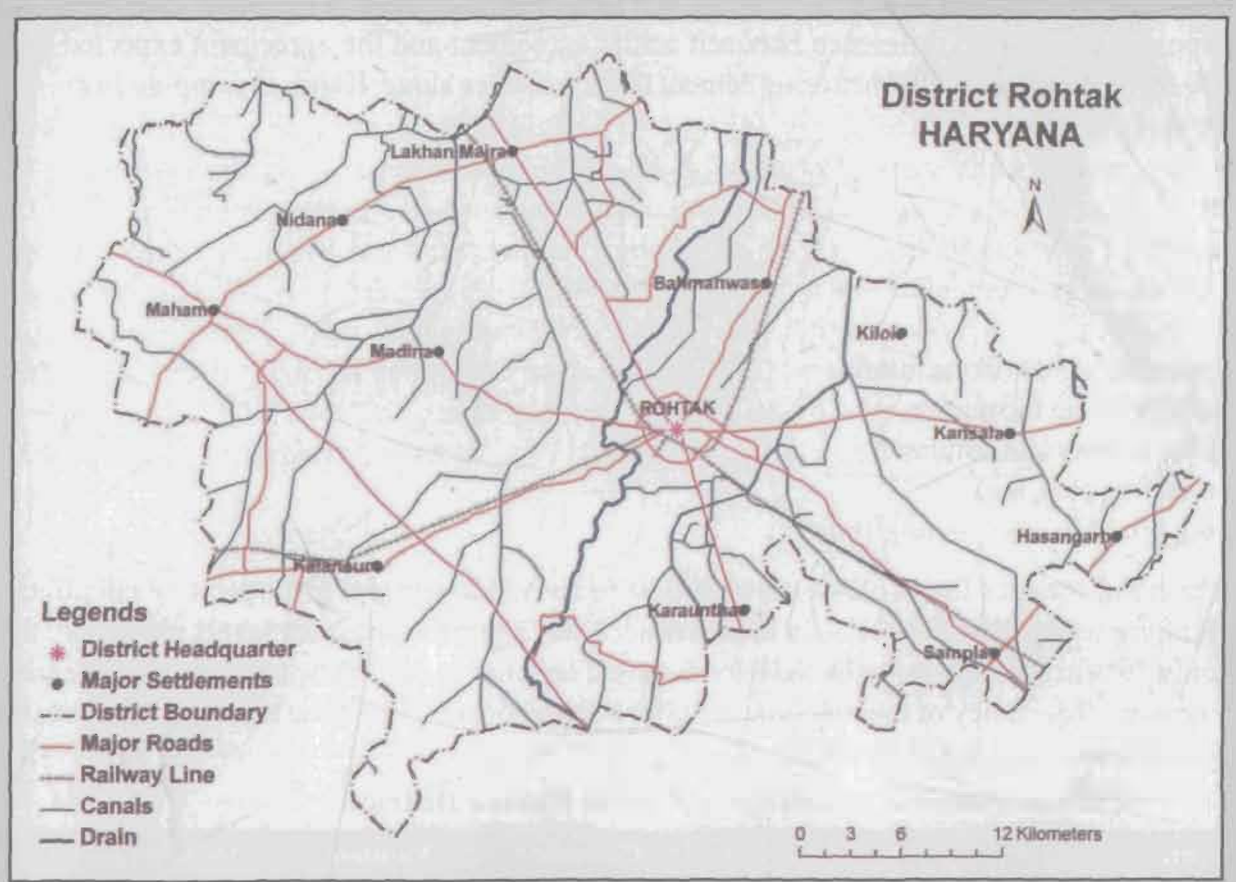

Fig. 5: Base map of Rohtak district.

The district falls in the Yamuna sub-basin of the Ganga basin, and is mainly drained by artificial drain No. 8 which flows from north to south. The natural vegetation of this region is dry deciduous scanty, xerophytic and widely dispersed. The most dominant of all trees, are the Acacia species (Acacia nilotica, Acacia tostilis), Jaal (Salvadora oleoides), Ber (Zizyphus maruitiana) and Shisham (Dalbergia Sisso). The major cropping system under the existing farming systems is primarily rice-wheat. The district has significant areas under other cropping systems of Arhar (kharif pulse) - wheat, sugarcane - sugarcane (ratoon)- wheat, jowar-wheat, vegetable-vegetable, vegetable-wheat, fallow-wheat, fallow-raya.

Extensive secondary salinisation is present in the canal irrigated area of 84193 ha. Despite the fact that drains have been constructed to manage the salinisation it is still a serious problem over much of the district. Soils are fine, to medium textured clay to sand over most of Rohtak, Sampla, and Lakhan Majra blocks whereas it is loamy sand with occasional clay loam in Kalanaur and Meham Blocks. The major soil associations at sub group level belong to Typic Torripsamments/ Ustipsamments/Ustorthents/ Ustifluvents/ Calciorthids/and Natric Cambiorthids.

Soil samples were collected from a 2km distance analysed and stored in non-spatial database of soil sample points. We generated a range in EC, pH values using the symbology tool of ArcGIS (Fig. 6). The spectral signature of each sample site was correlated with EC, pH values and other parameters. GPS readings collected during field work were converted to point data using ArcGIS 9.3.All vectors layers such as linear features canals, roads, drainage and soil sample point data were stored alongside in ArcGIS geodatabase.

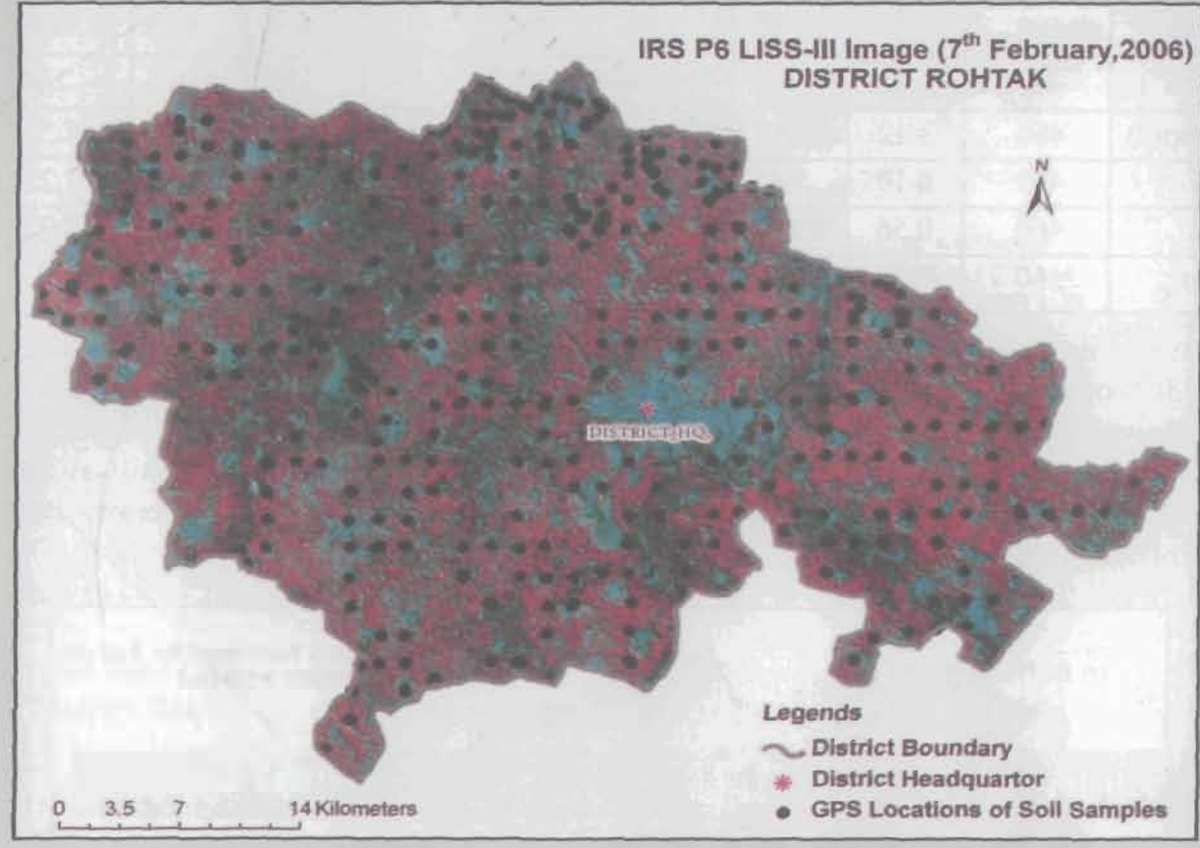

Fig. 6 : IRS-P6, LISS III satellite image and GPS location

Chemical properties of soil auger samples and geo-database structure analysis

In order to correlate ground soil analysis to the satellite images and to help build a suitable supervised classification NDVI, NDWI and SAVI models were applied to the 2km data (Table 3). A total of 460 soil samples were analysed to study their chemical properties (pH, EC & O.C.) macronutrient status (available P, K & S) and the micronutrients status (available Zn, Fe and Mn) were estimated. The pH of the soils ranged from 7.0 to 10.7 while the EC ranged from 0.1 to 20.0 dS m^{-1} indicating that the soils were both saline and saline-sodic in nature. On an average 75 and 90% of the soils had low fertility and contained 0.45% O.C. and 9.66 kg ha^{-1} of available P respectively (Table 4).

Only 25% of studied soils were deficient in available K with 114.0 kg ha^{-1}. Soils had sufficient amounts of available S whereas, 50% of the studied soil samples had medium levels of available Zn and Fe (0.88 and 5.77 mg kg^{-1} for available Zn and Fe, respectively) however only 25% of these samples had a

Table 4 : Summary of analysis of soil auger samples

Soil Property	No. of Analysed Samples	Min.	Max.	Avg.	S.D.	PERCENTILE				
						10th	25th	50th	75th	90th
pH	460	7	10.7	8.15	0.5	7.6	7.8	8.1	8.43	8.7
EC (dSm^{-1})	460	0.1	20	1.76	2.9	0.26	0.38	0.71	1.73	4.01
OC (%)	460	0.1	0.99	0.36	0.16	0.19	0.25	0.31	0.45	0.57
P_2O_5(Kg ha^{-1})	460	0.53	12.65	7.61	3.02	2	6.9	8.28	9.66	10.74
K_2O (Kg ha^{-1})	460	58	642	194.89	116.79	86	114	156.5	234	394.4
Sulpher (ppm)	460	3.12	617.7	151.62	138.78	17.75	49.92	103.73	218.57	359.11
Zn (ppm)	460	0.10	5.45	1.00	0.64	0.44	0.53	0.88	1.25	1.76
Fe (ppm)	460	0.56	23.72	6.65	3.76	3.03	4.14	5.77	8.32	11.17
Mn (ppm)	460	0.57	16.96	5.52	2.77	2.53	3.34	5.19	6.93	8.84

medium availability of Mn (3.34 mg kg^{-1}). The presence of degraded salt affected soils indicated that an estimated 30% of were intermittently saline and saline-sodic in nature and suffered from major deficiencies of O.C. and available P.

In order to preserve original values and prevent distortion the IDW algorithm was applied for generation of pH and EC maps. It was found that high pH and high EC soils were present over the district with most of the soils having a pH of 8 to 8.5 and an EC between 1-3 dSm^{-1} (Fig. 7 and Fig. 8)

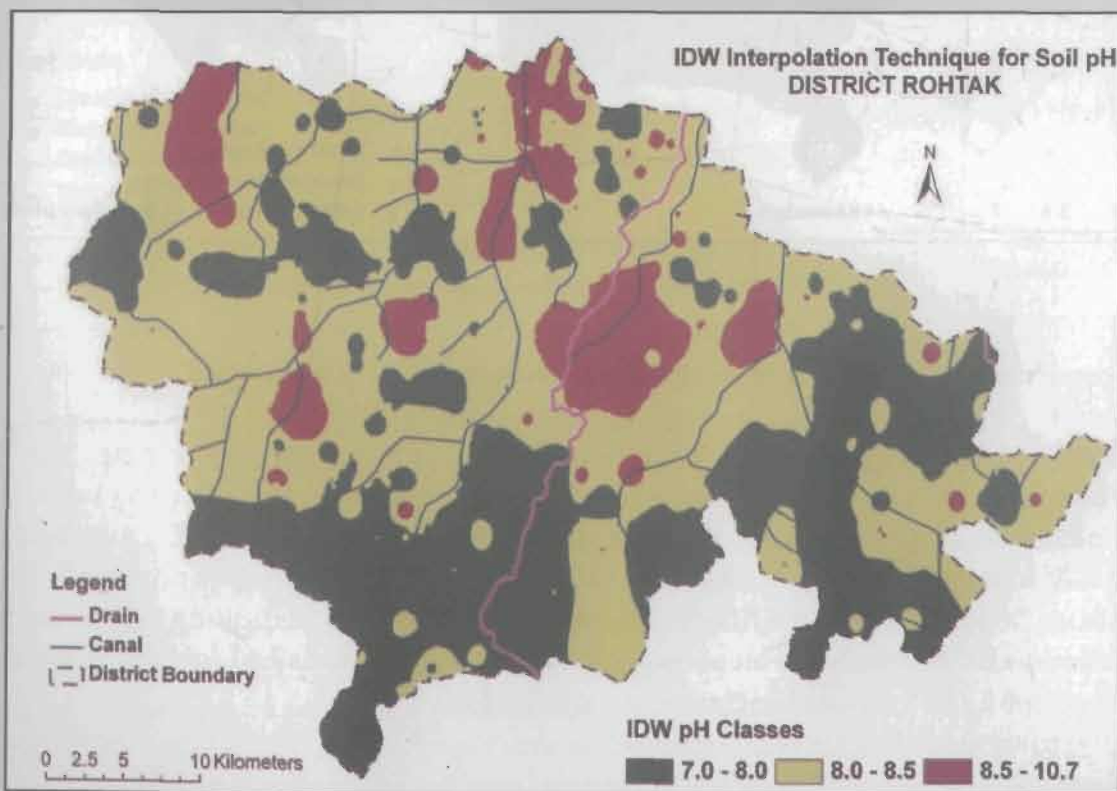

Fig. 7: IDW map of soil pH of Rohtak District

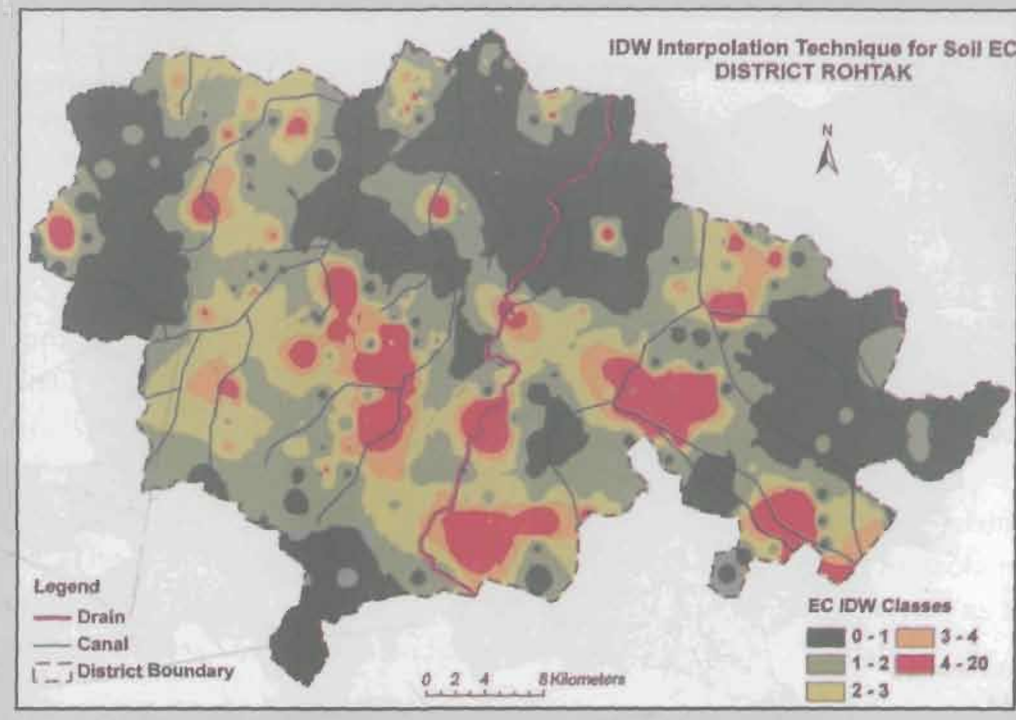

Fig. 8: IDW map of soil EC of Rohtak District

The supervised classification indicated that severely salt affected soils were found spread over 14100 ha area of district which was the 8.7% area of total geographical area of district. Moderately salt affected soils were found over ~54800ha (~34%) and sand dunes covered ~6100 ha (~4%) of the project area (Fig. 9). Moist soils with a possibility of high water tables and water logging was found over ~14200 ha found mainly in the vicinity of canals (Table 5).

Table 5: Area under different land cover classes based on supervised classification of District Rohtak Satellite Image

Land Cover Class	Area (ha)
Normal Soils/Agriculture	60107
Moderately salt affected soils with agriculture	54849
Severely salt affected/Barren	14058
Waterlogged and saline soils with agriculture	14224
Sand	6151
Waterbody	1917
Settlements	8940
Roads, canals & Others	14254
Total	**174500**

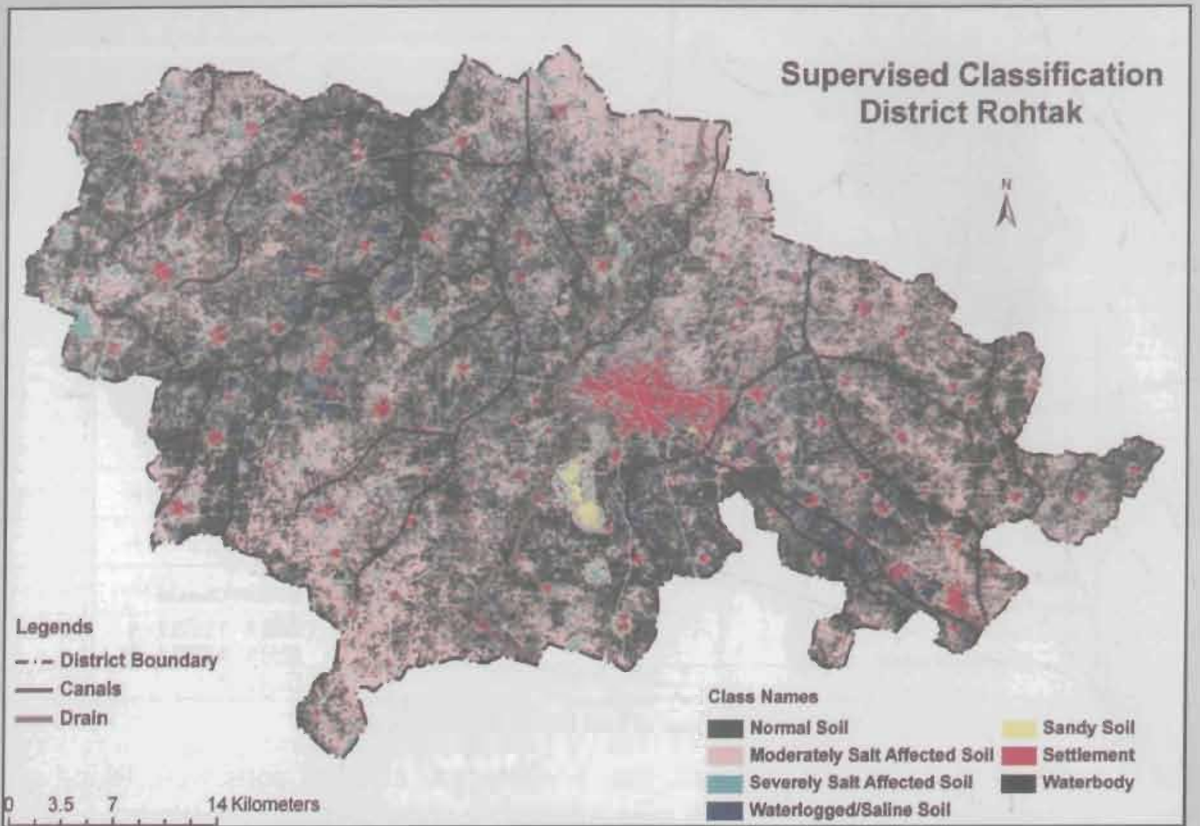

Fig. 9: Supervised classification map of IRS P6, LISS III satellite image of Rohtak District

BHIWANI DISTRICT

Bhiwani District is situated between 28° 11' 24" & 29° 3' 0" North latitude and 75° 15' 36" and 76° 16' 48" East Longitude (Fig. 10). The physiography of the district is mainly flat and level plain, interspersed by clusters of sand dunes, isolated hilocks and rocky ridges. The soils are largely sandy, sandy loam to loamy sand and taxonomically the soils belong to the sub groupe Typic Upstisamments, Typic Hpalustepts and Natric Haplustepts. The vegetation consists mainly of thorny trees like Babul(Aacia-Arabica), Jandi (Prosopis cineraria), Khair (Acacia catechu) along with Neem (Azadirachta indica), Shisham (Dalbergia sissoo), Peepal (Ficus religiosa), and crops like bajra, cotton in Kharif and wheat and mustard in Rabi. The area in the North east of the district is poorly drained and has considerable water logging and problems of salinity.

Soil samples were collected at 2 km distance. Satellite images were digitally enhanced, processed and georeferenced. The algorithms of the NDVI, NDWI and SAVI were applied for isolating salt affected soils and used as input for classification. Soil sampling was carried at 2km intervals as far as possible. Samples were collected from salt affected sites identified on the IRS images for analysis (Fig. 11).

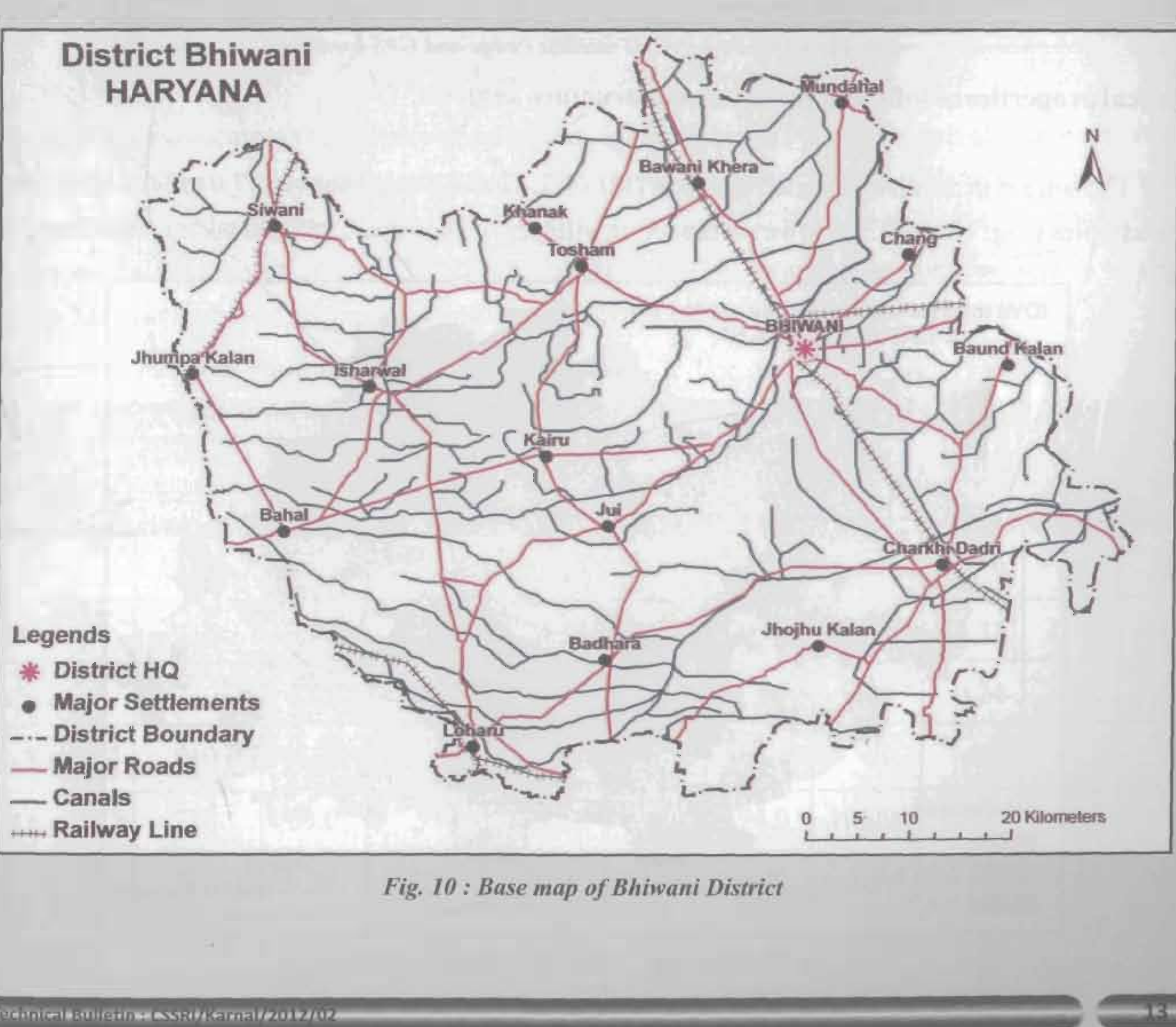

Fig. 10 : Base map of Bhiwani District

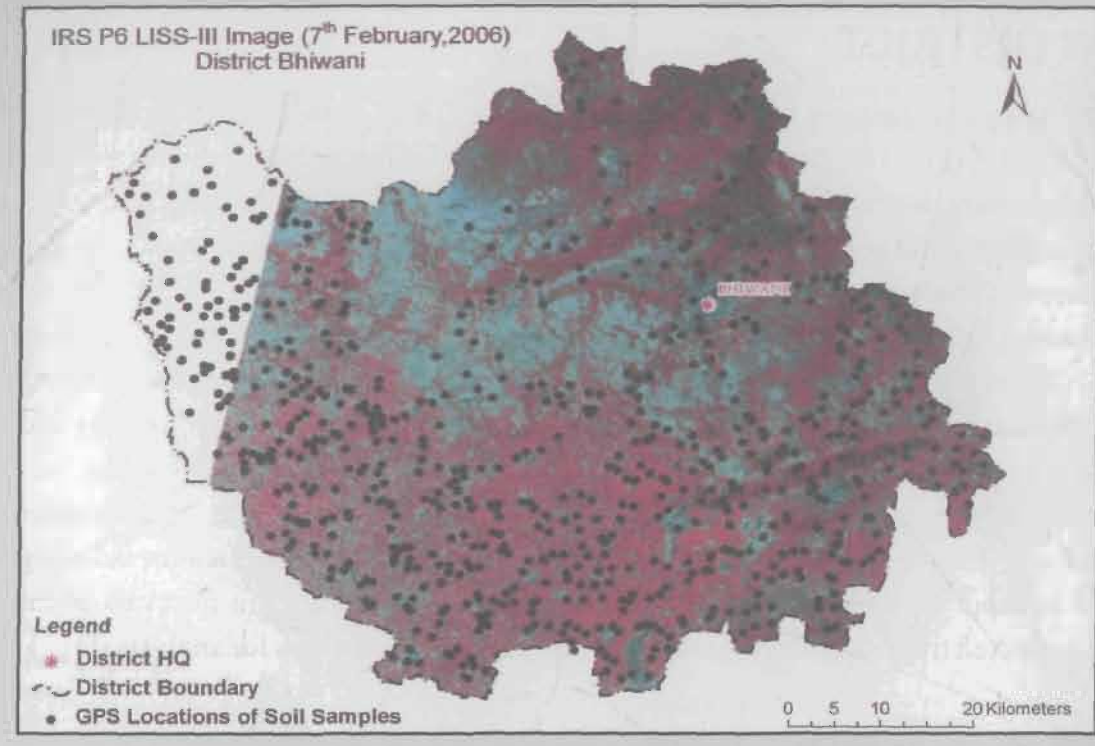

Fig. 11: – IRS P6 LISS III satellite image and GPS location

Chemical properties of soils and geo-database structure analysis

The soil pH in the district varied between 7.0 to 9.3. The EC varied between 7.0 to 31.0 dS m^{-1} in most of the samples (Fig. 12 and 13). However the EC in villages of Tigdana, Tigri, Ghuskani, and Chang were

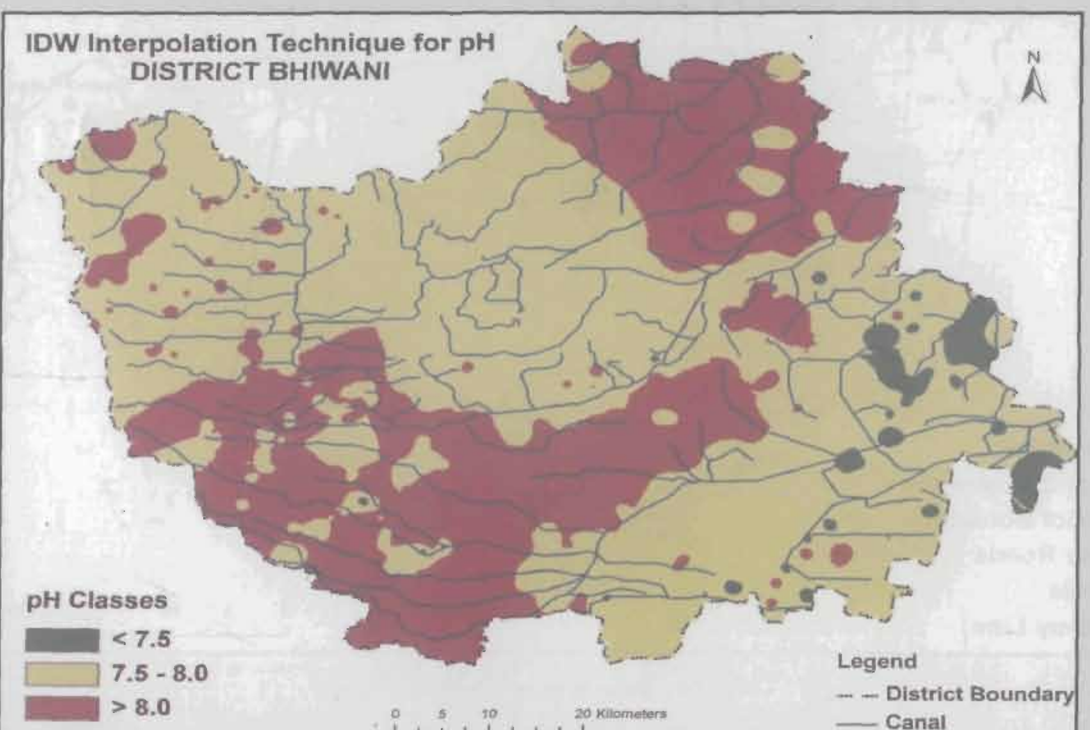

Fig. 12: IDW map of soil pH of Bhiwani District

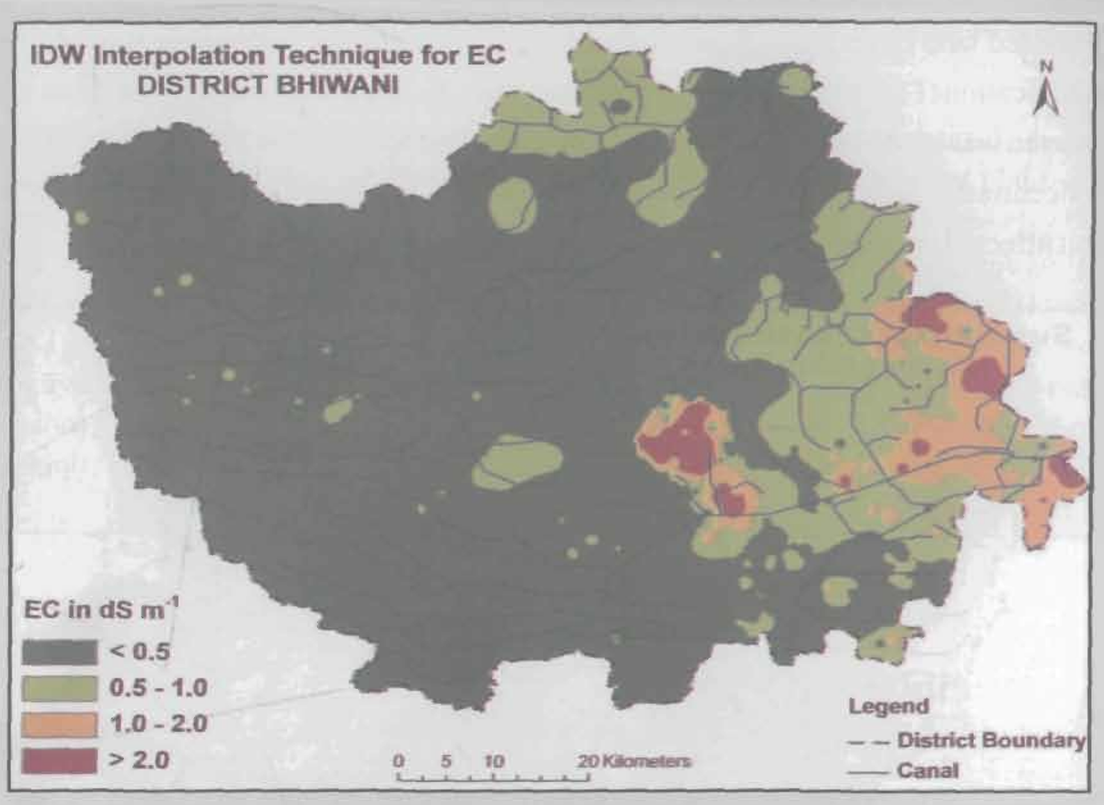

Fig. 13: IDW map of soil EC of Bhiwani District

relatively higher indicating the severity of salinity in the area. About 90% of the salt affected soils over the district were low in organic carbon with 0.36%. The availability of P_2O_5 in the soils was generally low and K_2O was available in moderate quantity in 75% of the soil samples with 144.0 kg ha^{-1}. About 25% of the soil samples are below the critical limit for Zn availability while Fe availability was low in 60% of the soil samples. Mn is available in sufficient quantities in 50% (5.2 mg kg^{-1}) of the soils (Table 6).

Table 6 : Soil analysis summary

Soil Property	No. of Analysed Samples	Min.	Max.	Avg.	S.D.	PERCENTILE				
						10th	25th	50th	75th	90th
pH	710	7.0	9.3	7.94	0.34	7.5	7.7	7.9	8.2	8.31
EC (dSm^{-1})	710	0.07	31.00	0.52	1.28	0.19	0.28	0.37	0.48	0.75
OC (%)	710	0.09	0.75	0.41	0.08	0.13	0.18	0.24	0.30	0.36
P_2O_5 (Kg ha^{-1})	710	1.10	20.00	6.81	3.71	2.0	4.0	6.3	8.1	10.5
K_2O (Kg ha^{-1})	710	60.0	994	130.12	50.9	94.0	106.0	122.0	144.0	164.2
Zn (ppm)	710	0.13	5.10	0.97	0.65	0.42	0.54	0.83	1.22	1.62
Fe (ppm)	710	1.08	13.7	4.16	2.06	2.03	2.84	3.62	5.07	7.22

A supervised land cover classification was carried out using the parametric rule and the maximum likelihood classification (Fig. 14). In total 7 land classes were distinguished of which the area under severely salt affected/barren was spread over 1.70% of the total classified area i.e. 464395 ha. Waterlogged and saline soils were concentrated mostly in the north eastern part of the district and covered 1.9% area while moderately salt affected soils covered (14.84%) of the total classified area (Table 7)

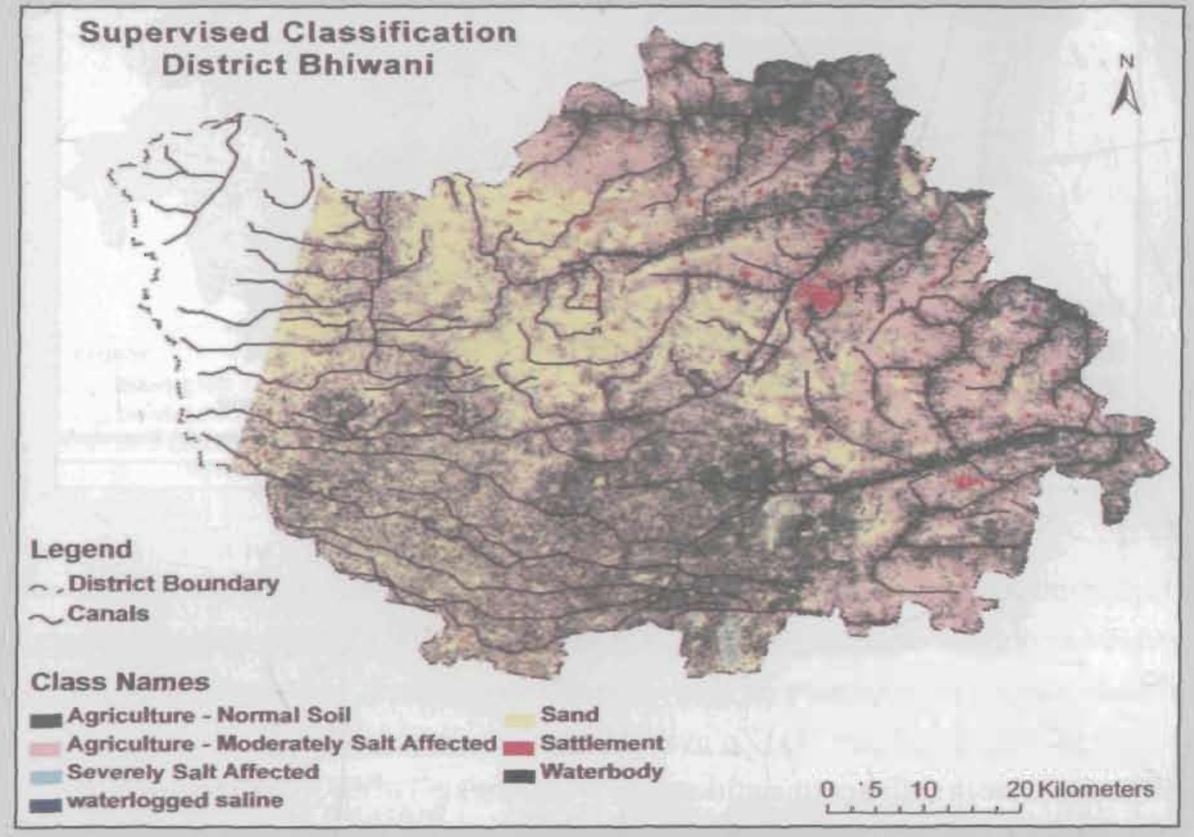

Fig. 14:- Supervised classification of IRS P6 LISS III satellite image of district Bhiwani

Table 7 : Area under different land cover classes based on supervised classification of Bhiwani district satellite image

Land Cover Class	Area (ha)
Normal Soils /Agriculture	119270
Agriculture- Moderately salt affected	68924
Severely salt affected/Barren	7891
Sand	201010
Waterbody	1194
Settlement	9878
Waterlogged and saline soils	8825
Roads, canals and Others	47403
Total classified area	464395
Area without image	45600
Total district area	**509995**

JIND DISTRICT

The District of Jind is located between 29°03' 00" to 29°51'00" North latitude and 75° 53' 00" to 76°45' 30" East longitude (Fig. 15). The physiography of the district is mainly flat plain with undulating sand dunes, sand ridges and depressions at places. The sand dunes/ridges are stable and may be at a height of 2 to 6 meters. The soils are largely are sandy loam to loam in texture. Taxonomically the soils belong to the subgroups of Typic Haplustepts, Fluventic Haplustept, Typic Ustipsamments, Natric Haplustepts, Typic Natustalfs and Typic Haplustalfs. The major crops grown in *Kharif* are paddy, cotton, bajra and fodder crops while wheat, raya and berseem are grown in the *Rabi* season. The natural vegetation is mainly Shisham (Dalbergia sissoo), Babul (Aacia-Arabica), Siris (Albizzia lebbeck), Neem (Azadirachta indica), and Jamun (Syzygium cumini). The north east and south east of the district is most affected by salinity.

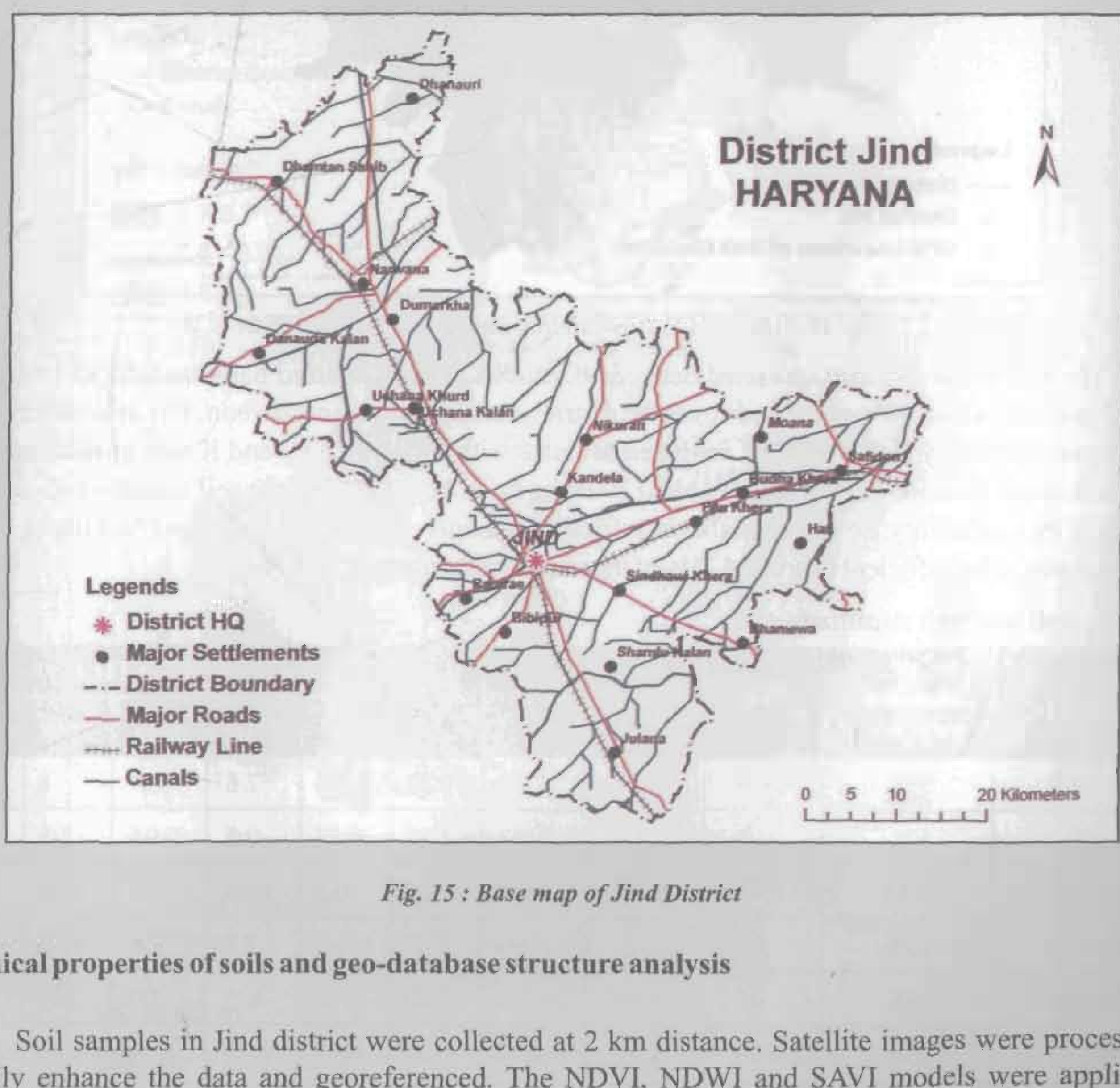

Fig. 15 : Base map of Jind District

Chemical properties of soils and geo-database structure analysis

Soil samples in Jind district were collected at 2 km distance. Satellite images were processed to digitally enhance the data and georeferenced. The NDVI, NDWI and SAVI models were applied for isolating salt affected soils and used for carrying out the supervised classification. Samples were collected from salt affected sites identified on the IRS images for analysis (Fig. 16).

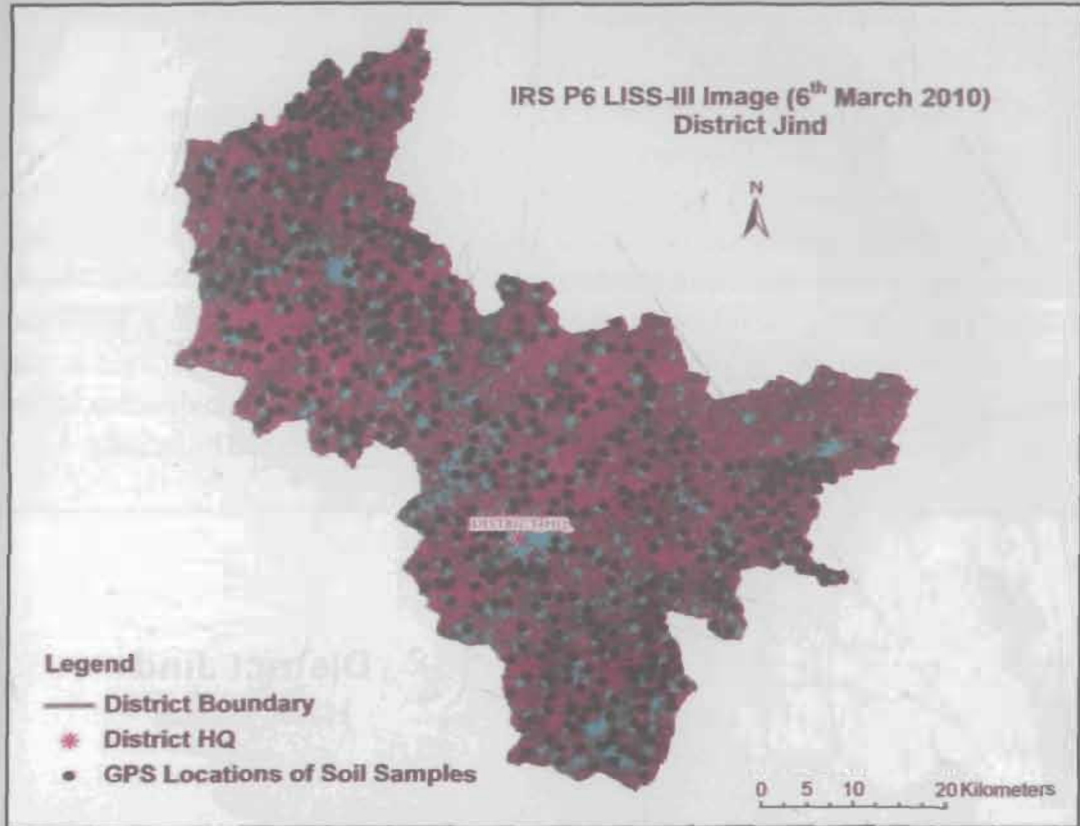

Fig. 16 : IRS P6 LISS III satellite image and GPS location

The soil pH in the district varied between 6.9 to 8.8. The EC varied between 0.08 to 10.0 d Sm^{-1} ((Fig.17 and 18). About 90% of the soils over the district were low in organic carbon. The availability of P in the soils was generally low (~90% of analyzed samples with 10.96 kg ha^{-1}) and K was available in good amounts in more than 50% of the soil samples (200.0 kg ha^{-1}). About 50% of the soil samples had sufficient quantity of Zn availability. Fe was available in sufficient amounts in 75% of the samples (9.68 mg kg^{-1}). Mn was also found to be sufficient in around 75% of the samples (7.36 mg kg^{-1}) (Table 8).

Table 8 : Soil analysis summary

Soil Property	No. of analysed samples	Min.	Max.	Avg.	S.D.	PERCENTILE				
						10th	25th	50th	75th	90th
pH	578	6.9	8.8	7.78	0.31	7.4	7.6	7.8	8	8.1
EC (dS m^{-1})	578	0.08	10	1.27	1.27	0.23	0.5	0.94	1.5	2.7
OC (%) 578	0.13	0.65	0.35	0.09	0.27	0.3	0.36	0.4	0.45	
P_2O_5 (Kg ha^{-1})	578	5.3	13.2	8.94	1.67	6.9	7.8	8.8	10.2	10.96
K_2O (Kg ha^{-1})	578	40	488	206.43	97.25	90	125	200	281	334
Zn (ppm)	578	0.18	5.37	1.12	0.65	0.49	0.59	1.05	1.43	1.93
Fe (ppm)	578	0.82	26.3	7.81	3.31	4.01	5.32	7.64	9.68	11.52
Mn (ppm)	578	2.09	25.86	7.69	3	4.27	5.64	7.36	9.28	11.3

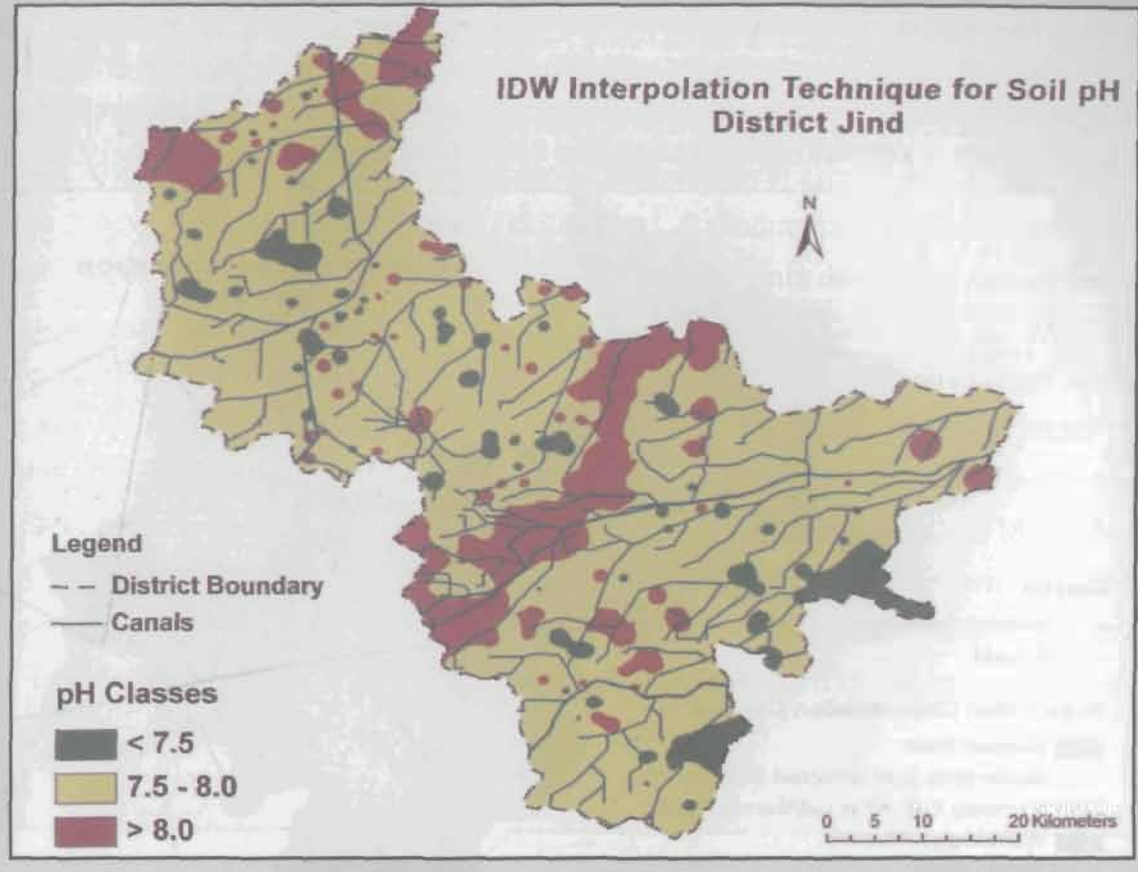

Fig. 17 : IDW map of soil pH of district Jind

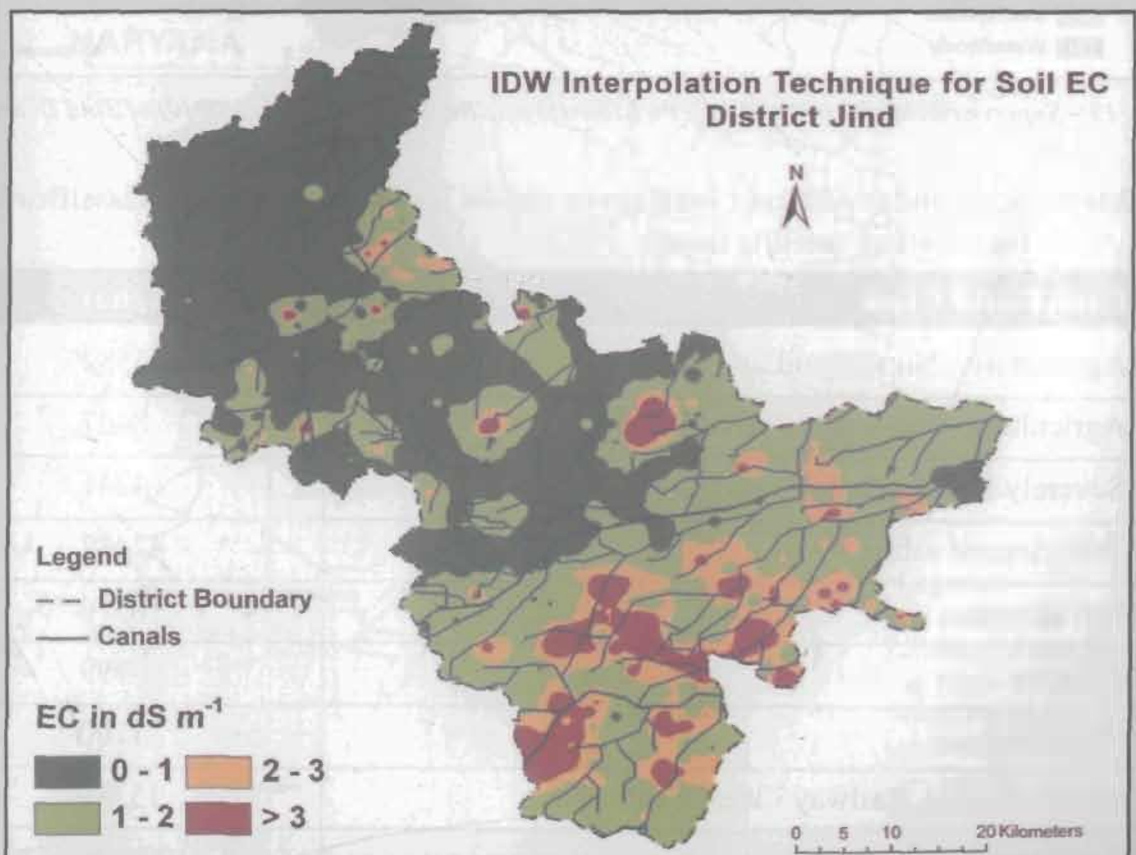

Fig. 18 : IDW map of soil EC of district Jind

Using the parametric rule maximum likelihood supervised classification 8 land classes were distinguished of which the area under severely salt affected/barren soils was found over 1.54% of the area and moderately salt affected soils covered13.9% of the total area (Table 9). Waterlogged and saline soils were concentrated mostly in the north eastern part of the district and covered 4.50% (Fig. 19).

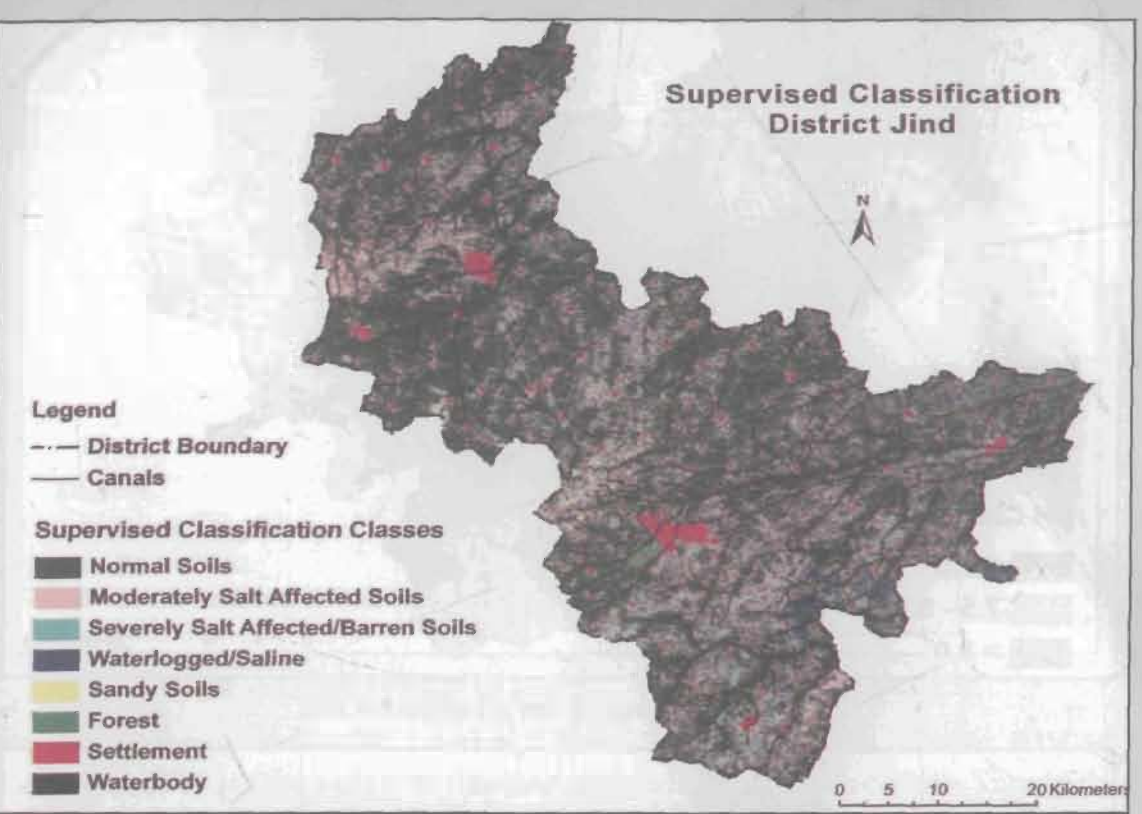

Fig. 19:- Supervised classification of IRS P6 LISS-III satellite image (6th March 2010) of Jind District

Table 9 : Area under different land cover classes based on supervised classification of Jind district satellite image

Land Cover Class	Area (ha)
Agriculture - Normal soil	95582
Agriculture - Moderately salt affected	8407
Severely salt affected / barren	4241
Waterlogged saline	42432
Settlements	8576
Forests	499
Waterbody	1100
Others (Roads, Railway Lines, Canals etc.)	15389
Total	**276226**

JHAJJAR DISTRICT

Jhajjar district is located between 28 ° 33' N and 28 ° 42' N latitude and 76° 28' 45" W and 76 ° 84' 15" E longitude (Fig. 20). The district is divided into three tehsils namely Jhajjar, Bahadurgarh and Beri. Further subdivided into 5 development blocks namely Jhajjar, Beri, Bahadurgarh, Matenhail and Salahwas. The district also falls in the Yamuna sub-basin of Ganga basin, and is mainly drained by the artificial drain No.8 flowing from north to south. Jawahar Lal Nehru feeder and Bhalaut sub Branch are main canals of the district. The geomorphology is mainly alluvial plain and undulating dunes with an average elevation of 222 meters above sea level. The sediment is made up of sand, silt, clay, gravel and calcium carbonate at shallower depths. The soils of the district are coarse to medium textured. It comprises sand to sandy loam in north eastern part covering Bahadurgarh, and Jhajjar blocks. The soil of Sahlawas and Mattanhail Block are sandy to sandy loam in texture. The soil contains massive beds of pale reddish brown coloured clay in the southern eastern parts of the area. The area is composed of arid region Aridisols such as Cambiorthids and Calciorthids. Taxonomically the soils are mainly TypicHaplustepts, Typic Ustipsamments and Typic Ustorthents.

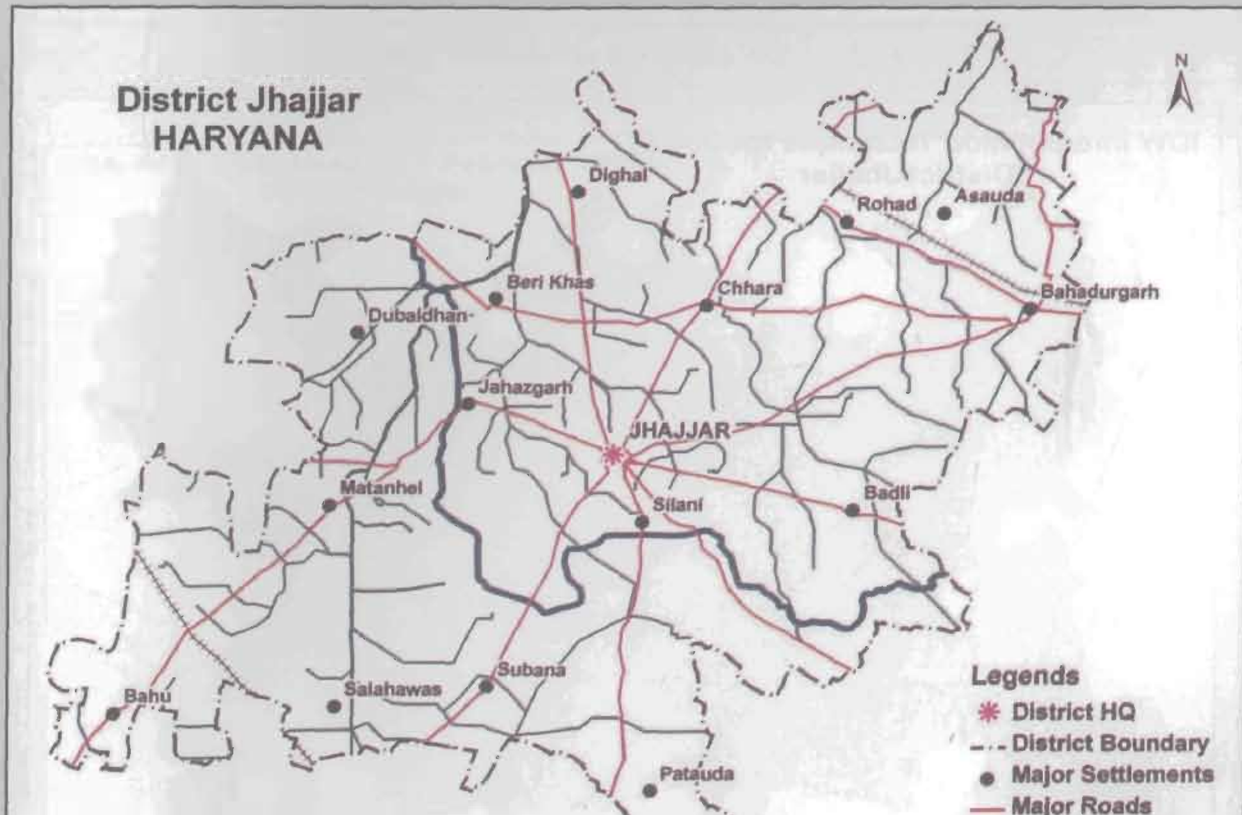

Fig. 20: Base map of Jhajjar District.

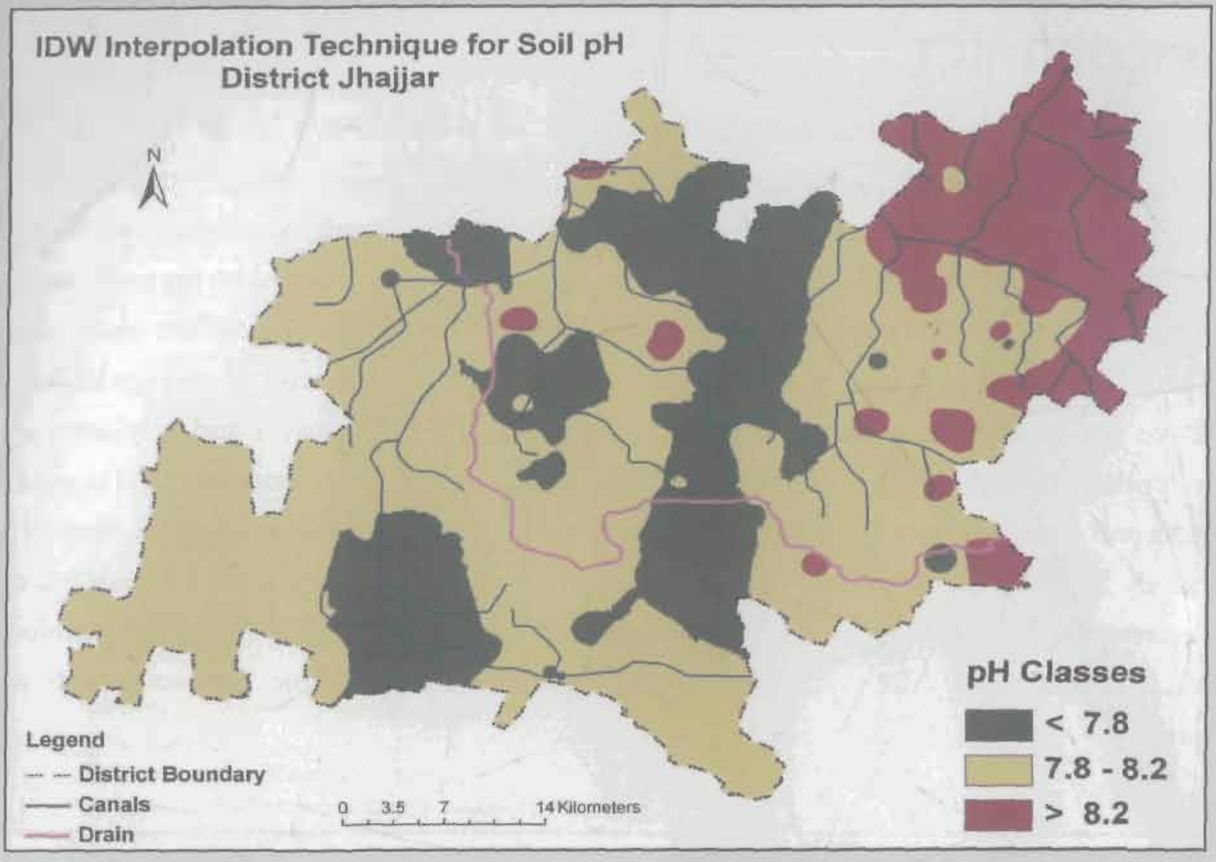

Fig. 21 : IDW map of soil pH of district Jhajjar

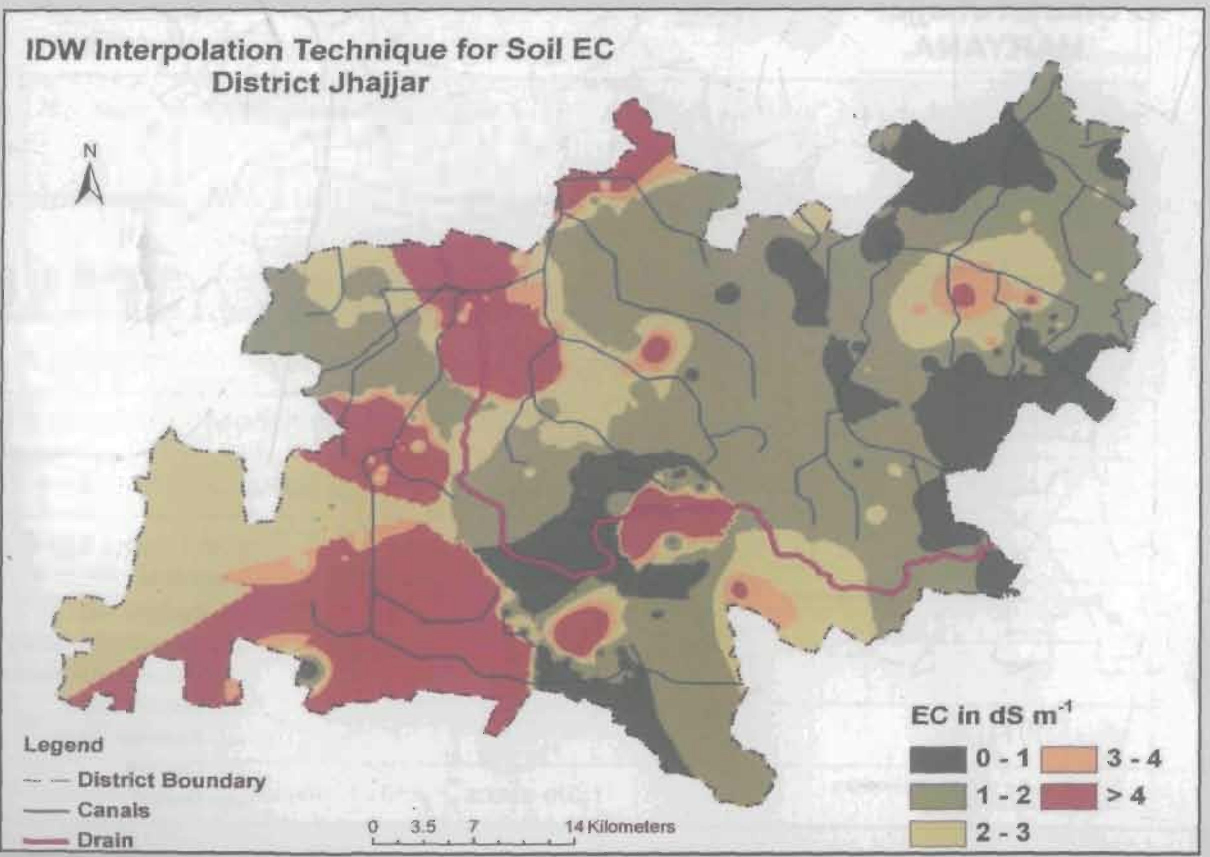

Fig. 22 : IDW map of soil EC of Jhajjar District

Chemical properties of soils and geo-database structure analysis

The pH of the soils ranged from 6.7 to 9.3 and the EC ranged from 0.69 to 99.4 dS m^{-1} (Fig. 21 and 22) ranging from saline to sodic. This information along with other parameters of Na, K, Ca and Mg were

Table 10 : Soil analysis summary

Soil Property	No. of Analysed Samples	Min.	Max.	Avg.	S.D.	PERCENTILE				
						10th	25th	50th	75th	90th
pH	466	7	9	7.89	0.36	7.4	7.7	7.9	8.1	8.4
EC (dS m^{-1})	466	0.1	5.1	1.21	0.87	0.2	0.52	1	1.7	2.4
OC (%)	466	0.1	0.45	0.22	0.06	0.16	0.18	0.21	0.26	0.28
P_2O_5 (Kg ha^{-1})	466	1.62	9.3	4.07	1.83	2.04	2.47	3.9	5.4	6.6
K_2O (Kg ha^{-1})	466	16	440	127.11	63.86	63	80	123	170	188
Sulpher (ppm)	188	18.41	218.4	96.8	35.72	55.85	65.75	92.35	119.03	137.62
Zn (ppm)	466	0.11	2.7	0.79	0.38	0.43	0.52	0.63	1.05	1.3
Fe (ppm)	466	0	14.7	5.47	2.17	2.91	4.03	5.23	6.5	8.43
Mn (ppm)	466	2.14	17.4	6.72	2.49	4.06	4.82	6.26	7.84	9.85

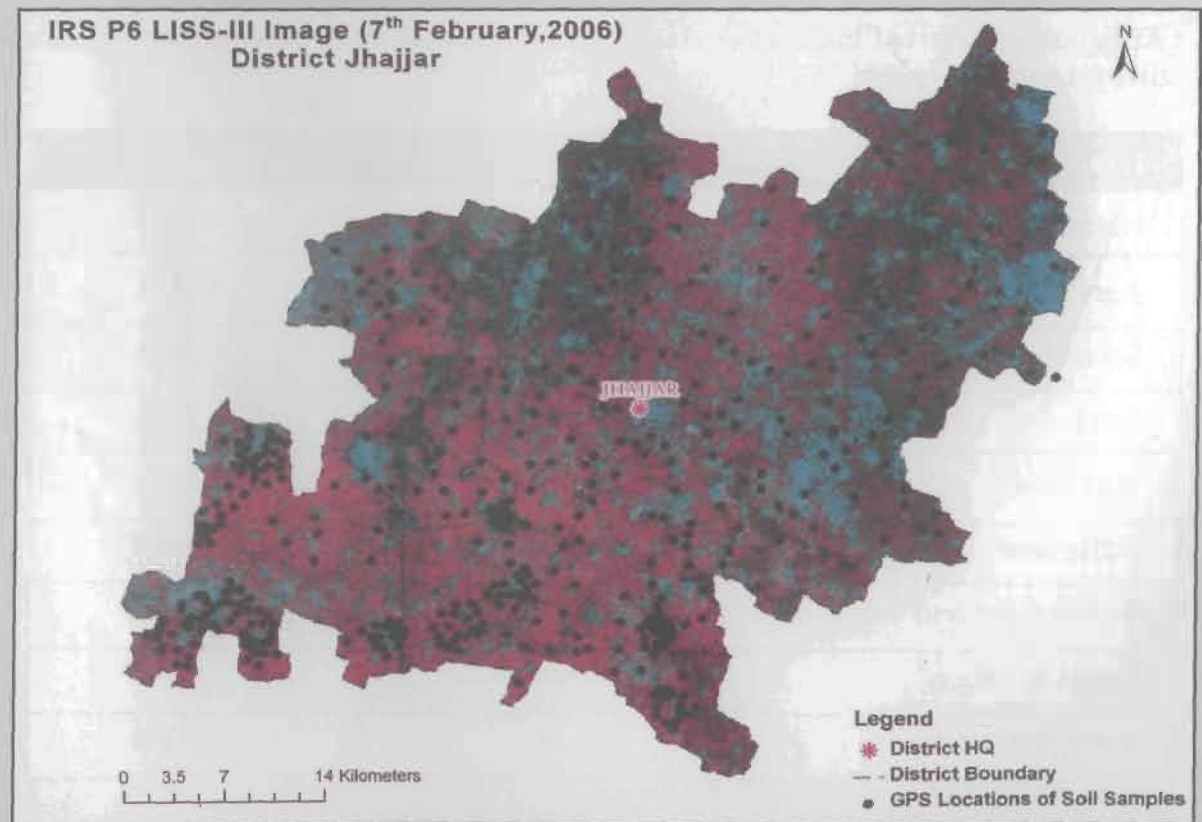

Fig. 23: IRS P6 LISS III satellite image and GPS location

transferred into ArcGIS for processing and training the computer. Both salinity and waterlogging were identified on the images and the soils were found to be deficient in micronutrient (available N and P) and micronutrient Zn. On an average 90% of the soils had low fertility and contained 0.28% of O.C. and 6.6 kg ha^{-1} of available P, respectively (Table 10).

Spectral signatures of each sample site were examined on satellite image (Fig. 23). The ISODATA algorithm was used to run initial iterations to cluster the pixels into similar classes. The classes were again iterated to create a lesser number of clusters. 6 X 6 pixels for each class was then isolated across the district based on spectral signature for establishing groups. Training sites were decided for different classes for classification to run the maximum likelihood algorithm for creating a supervised classified image for the District.

A total of eight classes sand, severely salt affected/barren, moderately salt affected, waterlogged and saline soils, settlement, normal soils/agriculture and water bodies identified and these were basis for training sites (Table 11). The salt affected classes of severely salt affected/ barren soils were most straightforward to map covering an area of 15953ha. Moderately salt affected lands supporting agriculture covered an area of 62158 ha. Waterlogged and saline soils were found in over 129.87ha. Normal Soils with agriculture were spread over 82623 ha over the district. The rest of the area was classified into water bodies, settlements, sand and other categories. An accuracy assessment was carried out and an accuracy of 8725 is indicative that the methodology adopted has a high level of applicability in the assessment of salt affected soils (Fig. 24).

Table 11 : Area under different land cover classes based on supervised classification of Jhajjar district satellite image

Land Cover Class	Area (ha)
Normal Soils/Agriculture	82623
Agriculture-Moderately salt affected	62158
Severely salt affected/barren	15953
Sand	7416
Waterbody	1809
Settlement	8444
Waterlogged and saline soils	12987
Roads & Others	7000
Total district area	**198390**

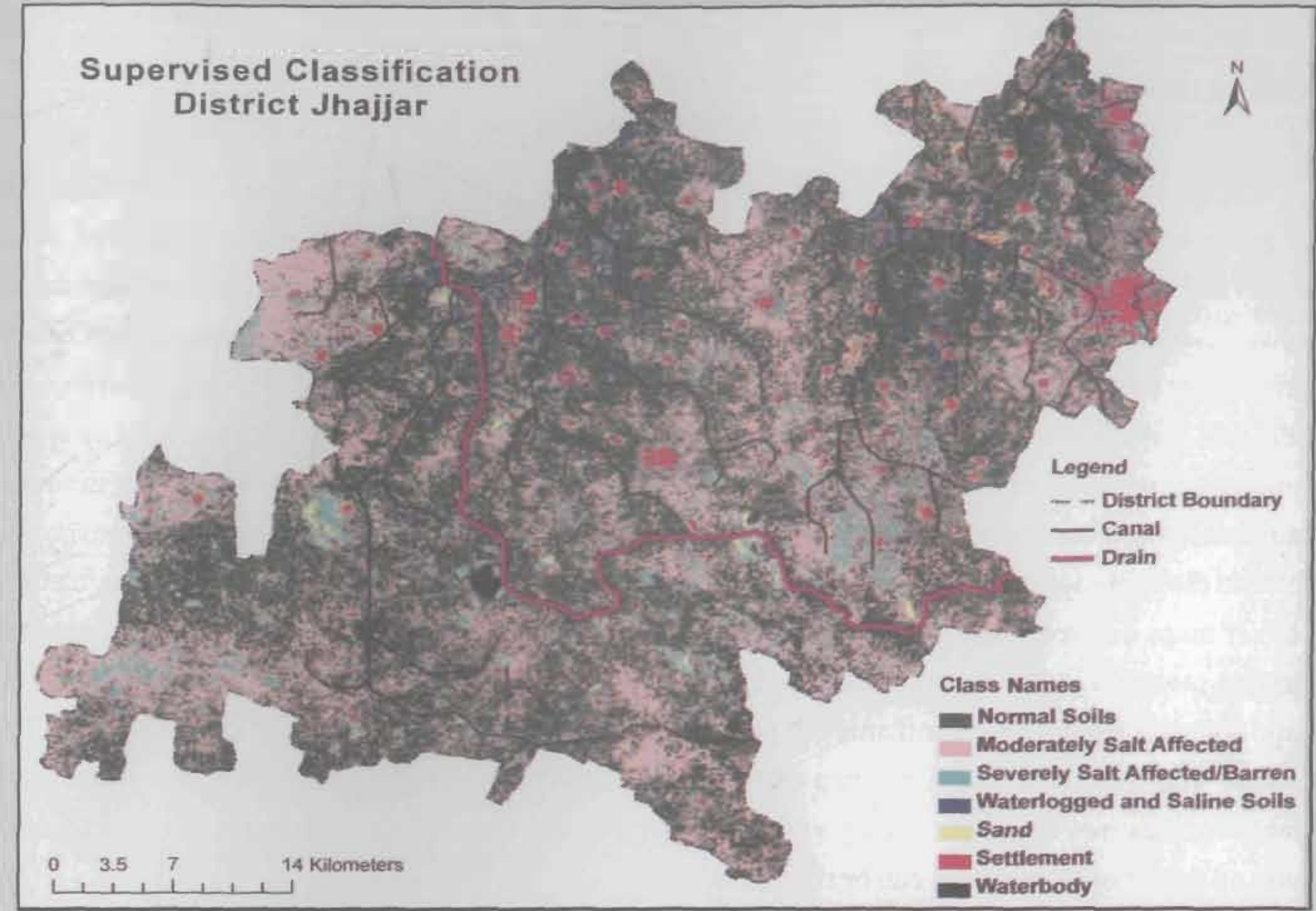

Fig. 24 : Supervised classification of Jhajjar District

CONCLUSIONS

The detailed methodology involved contains a stepwise efficient system in sequence that includes initial interpretation and processing of image data, ground truth using GPS and subsequent sample collection and analysis. Indices were used to extract information and provide input the classification. The supervised classification and its accuracy assessment is indication that the presented methodology is robust and simpler for detecting degraded salt affected soils in other districts of Haryana. Ground truth remains an essential and imperative input. Soil analysis remains necessary to establish the salt affected status of the soils and it is not possible to differentiate salinity from alkalinity. This remains a drawback of the remote sensing technique. The ability to study spectra in different bands and correlate them to ground truth provides insight into the accuracy of the different classifications and mapping. The accuracy of the classification of land-cover maps derived from LISS-III data were found to be 87.25 % which indicates that the sequential system that included initial interpretation and processing of image data, ground truth collection using the GPS and soil sample collection and analysis and application of the supervised classification technique was successful. The increased ability to map degraded salt affected soils would enhance the probability of reclamation measures being put into place. Monitoring could become more frequent and over time the process and extent of degradation can be monitored

Further accuracies could be achieved for salt affected soils using improved software and sub pixel classification for more precise validation in future (Srinivasan and Richards, 1990; Arora and Foody, 1997; Binaghi et al. 1997; Arora and Mathur, 2001).

ACKNOWLEDGMENT

The team expresses gratitude to Director, CSSRI for providing the finance and the necessary infrastructure for the project. We appreciate the support and help of Head, Division of Soils and Crop Management. We are grateful to Mr. Naresh Arora and Mr. Kashmir Singh for all their assistance in cataloguing, processing and analysis of soil samples. We are indebted to all the staff of the Soil Testing Laboratory, Karnal, who helped in collection of data. We thank our reviewers for their valuable comments. Most of all we thank the farmers we met during this journey who provided us the information and guided our path.

REFERENCES

Ackerman, T., Erickson, T. and Williams, M.W., 2001, Combining GIS and GPS to Improve Our Understanding of the Spatial Distribution of Snow Water Equivalence (SWE). *ESRI Users Conference*. San Diego, California.

Arora MK, Foody GM. 1997. Log-linear modeling for the evaluation of variables affecting the accuracy of probabilistic fuzzy and neural network classifications. *International Journal of Remote Sensing* **18(4)**, 785–798. DOI: 10.1080/014311697218755

Arora MK, Mathur S. 2001. Multi-source classification using artificial neural networks in a rugged terrain. *Geocarto International*. **16(3)**, 37–44. DOI: 10.1080/10106040108542202

Binaghi E, Madella P, Montesano MG, Rampini A. 1997. Fuzzy contextual classification of multisource remote sensing images. *IEEE Transactions on Geoscience and Remote Sensing* **35(2)**, 326–340. DOI: 10.1109/36.563272

Congalton R. 1991. A review of assessing the accuracy of classifications of remotely sensed data. *Remote Sensing of Environment*. **37**, 35–46. DOI: 10.1016/0034-4257(91)90048-B

Jensen JR. 1996. Introductory Digital Image Processing: *A Remote Sensing Perspective* (Second edition). Prentice Hall, Inc., Upper Saddle River, New Jersey.

Lu D, Li G, Valladares GS, Bastitella M. 2004. Mapping Soil erosion risk in Rondônia, Brazilian Amazonia: using RUSLE, remote sensing and GIS. *Land Degradation & Development* **15**: 499–512. DOI: 10.1002/ldr.634

Madrigal LP, Wiegand CL, Meraz JG, Rubio BDR, Ramı´rez OL. 2003. Soil salinity and its effect on crop yield: A study using satellite imagery in three irrigation districts. *Ingenieria Hidraulica en Mexico* **18**: 83–97.

Menenti M, Lorkeers A, Vissers M. 1986. An application of Thematic Mapper data in Tunisia. *ITC Journal* **1**: 35–42. DOI: WebQuery/wurpubs/127

Metternicht GI, Zinck JA. 2003. Remote sensing of soil salinity: Potentials and constraints. *Remote Sensing of Environment* **85**: 1–20. DOI: 10.1016/S0034-4257(02)00188-8

Racoviteanu AE, Manley WF, Arnaud Y, Williams M. 2007. Evaluating digital elevation models for glaciologic applications: An example from Nevado Coropuna, Peruvian Andes. *Global Planet Change* **59**, pp. 110-125. DOI: 10.1016/j.gloplacha.2006.11.036

Richards JA. 1999, *Remote Sensing Digital Image Analysis: An Introduction,* Springer-Verlag, Berlin, Germany, 240 p.

Saha SK, Kudrat M, Bhan SK. 1990. Digital processing of LANDSAT TM data for wasteland mapping in parts of Aligarh District (Uttar Pradesh), India. *International Journal of Remote Sensing* **11(3)**: 485–492. DOI: 10.1080/01431169008955034

Srinivasan A, Richards JA. 1990. Knowledge-based techniques for multisource classification. *International Journal of Remote Sensing* **11(3)**, 505–525. DOI: 10.1080/01431169008955036

Sharma RC, Bhargava GP. 1988. LANDSAT imageries for mapping saline soils and wetlands in north-west India. *International Journal of Remote Sensing* **9**: 39–44. DOI: 10.1080/01431168808954835

Sethi M, Ghosh DK, Kudrat M. 2001, Inventorying salt-affected soils a case study of Kanpur District Uttar Pradesh, India. In: *Spatial Information Technology, Remote Sensing and Geographical Information Systems*, vol. **II**, I.V. Muralikrishnan (Ed.), pp. 417–422 (Hyderabad, India: ICORG, BS Publications).

Sethi M, Gupta SK, Dubey DD. 1996. Assessment of soil salinity and waterlogging in the Ukai–Kakrapar command area using remotely sensed data. In: *Proceedings of Workshop on Ukai Kakrapar Command Area*, Anand, Gujarat, pp. 56–63.

Sethi M, Sharma BD, Kumar R, Lal K, Gupta SK. 2004. Prognosing Secondary Salinization in a part of an irrigated command area of south west Punjab, India. *NATP Final report* (World Bank).

Singh G, Bundela DS, Sethi M, Lal K, Kamra SK. (2009) Remote Sensing and Geographic Information System for Appraisal of Salt-Affected Soils in India. *Journal of Environmental Quality* **39**:5-15. DOI:10.2134/jeq2009.0032

Venkataratnam L. 1980. Delineation and mapping of agricultural soil limitations/hazards in arid and semi-arid tropics using LANDSAT- MSS data: An Indian experience, pp. 905-914 in *Proceedings 14th International Symposium on Remote Sensing of Environment*, Ann Arbor, MI

www.crisp.nus.edu.sg/~research Optical Remote Sensing - Principles of Remote Sensing

Technical Bulletin :
CSSRI/Karnal/Bulletin/2012/02